“Calcium dynamics and compartmentalization in leech neurons”

Thesis submitted for the degree of “Doctor Philosophiae”

CANDIDATE
Sofija Andjelic

SUPERVISOR
Prof. Vincent Torre

To all that I love

Table of contents

Acknowledgements

First of all, I wish to express my gratitude to Prof. Vincent Torre for his support and for carefully supervising my PhD work.

I thank Prof. John Nicholls for all he taught me and for his precious advice.

I thank all my colleagues and friends. I'm especially grateful to Walter Vanzella who assisted in the development of the software for image analysis, to Paolo Bonifazi who assisted in the preparation of the figures, and to the members of the "leech " group Elisabeth Garcia Perez and Alberto Mazzoni for useful discussions and collaboration.

Note

The work described in this thesis dissertation was carried out at the International School for Advanced Studies, Trieste, between November 2001 and December 2005. All work reported arises solely from my own experiments and has not been submitted, as in whole or in a part, to any other University.

Sofija Andjelic

Abbreviations used in the text

σ: standard deviation

AE: annulus erector motoneuron

AP: action potential

CNS: central nervous system

CV: coefficient of variation

ΔF/F: fractional change in light intensity

1 Preface

Animals are continually exposed to the changes in their environment, which they must detect through sensory receptors. Mechanical or chemical stimulation, heat, light, are just some of the inputs that change. The brain is able, by highly complex neural mechanisms, to integrate the inputs and generate appropriate responses. The output commands represent decisions made by the brain and transmitted to effector cells, so that life can continue. From invertebrates to higher vertebrates, all different forms of life use similar types of information processing and signal integration to survive. The numbers of cells increase with evolution, but the principles remain the same, or at least appear to do so. To understand more information processing and integration, we have chosen to investigate the leech nervous system. For these experiments we have decided to study the role of single identified nerve cells of the leech in information processing and integration, because previous studies have provided much detailed information about their morphological, physiological and functional properties.

To what extent is it useful to understand leech neurons? While Nietzche in "Also sprach Zarathustra" said that it was a worthy ambition to be a master of the leech's brain, others might be satisfied only by understanding the human brain.

Nevertheless, nature with all its vast diversity does exist even if we do not understand it. If deepening our understanding makes us admire it even more, then science is art, the art of celebrating beauty, the beauty of perfection.

Abstract

The aim of this project was to study how and where action potentials arise and propagate in the arborizations of identified neurons in the central nervous system of the leech. A major aim was to assess whether the entry of calcium is localized to distinct regions of the cells and to determine whether there are significant differences in calcium channel distribution between different types of neurons.

A combination of electrophysiological techniques, optical recording and image analysis was used to approach these problems. I developed an experimental set-up for optical recordings of calcium transients by a fast CCD-camera. By use of calcium sensitive dyes I analysed in detail optical responses to electrical stimulation of neurons and the density of calcium channels, spatially and temporarily, in different neural cell types, including mechanosensory neurons and motoneurons. Fluorescence changes ($\Delta F/F$) of the membrane impermeable calcium indicator Oregon Green were measured. The dye was pressure injected into the soma of neurons under investigation. $\Delta F/F$ caused by a single action potential (AP) in mechanosensory neurons had approximately the same amplitude and time course in the soma and in distal processes. By contrast, in other neurons such as the Anterior Pagoda neuron, the Annulus Erector motoneuron, the L motoneuron and other motoneurons, APs evoked by passing depolarizing current in the soma produced much larger fluorescence changes in distal processes than in the soma. When APs were evoked by stimulating one distal axon through the root, $\Delta F/F$ was large in all distal processes, but very small in the soma. These results confirm and extend previous electrophysiological data which demonstrate that the soma of a motoneuron in the leech, as in many other invertebrates, does not generate action potentials (Stuart, 1970; Muller and Nicholls,

1974; Goodman and Heitler, 1979). Impulses recorded in the soma are normally only a few millivolts in amplitude. The AP of a motoneuron propagates to muscles of the body wall along segmental nerves that emerge from ganglia. The site of impulse initiation has been found to be at a distance from the soma but within the ganglion (Melinek and Muller, 1996; Gu et al. 1991). Our experiments with fluorescent transients are in accord with the concept that they result from calcium entry through voltage sensitive channels. Thus at sites where APs are found to be large, the calcium signals are large (as in peripheral axons), while at sites where spikes are small, (as in motoneuronal cell bodies) signals were weak, or non existent.

Our results show a clear compartmentalization of calcium dynamics in leech neurons in which the soma does not make propagating action potentials. Such cells represent interneurons as well as motoneurons and constitute the vast majority of ganglion cells. In such cells, although the soma is not excitable it can affect information processing by modulating the sites of origin and conduction of AP propagation in distal excitable processes.

1 Introduction and background

Understanding the biophysical properties of single neurons and how they process information is fundamental for understanding complex integrative mechanisms of the brain. Early classical models of neurons were based on the assumption that dendrites behave as purely passive electrical elements. Recent studies have however shown that active regional electrical properties of individual neurones are extraordinarily complex and dynamic and that functional organisation of a neuron depends on variable distributions of voltage-gated channels. The principles of information processing in single neurons can only be determined by studying specific neuronal types in different experimental preparations.

Many studies have been carried out using invertebrate neurons, primarily because of the ease with which their intrinsic properties can be analysed and related to animal behaviour. One can study how the brain of an invertebrate, which is made up of ganglia with their limited numbers of cells, generates all its movements, avoidance, hesitations, feeding, mating, and sensations. The remarkably stereotyped morphological appearance, together with the large size of the neuron cell bodies, make segmental ganglia of the leech ideal preparations for identifying the functions of individual cells and for studying their physiological properties (Muller et al, 1981).

Since biophysical properties of neurons in mammals and invertebrates are rather similar, the understanding of information processing in simple nervous systems provides a basis for unravelling mechanisms used by the brains of higher animals.

In my PhD project, I have used a combination of optical and intracellular recording and image analysis to investigate calcium dynamics and compartmentalization in mechanosensory

neurons and motoneurons of leech *Hirudo medicinalis*. For the analysis of problems concerned with signalling, optical recording techniques using appropriate indicator dyes can provide a sensitive assay with high temporal and spatial resolution. Optical responses to electrical stimulation of a neuron were studied in detail, spatially and temporarily, in different neural cell types. In this way, I have indirectly investigated the distribution of calcium transients and compartmentalisation in these neuronal types.

For studying signal integration, AP initiation and propagation by using optical techniques, which have good spatial resolution, an obvious choice would be the use of the voltage-sensitive dyes. We have some preliminary results with these dyes and they will be discussed in chapter 5. A problem with these dyes however is low signal to noise ratio, and as a result, signals are often very small and masked by noise.

In this introductory chapter I provide the rationale and the background of my thesis. Basic information about the neurobiology of the leech is presented in section 1.1. In section 1.2 the issue of functional organisation of neural cell is reviewed with the focus on calcium dynamics. Important publications on calcium dynamics and electrical compartmentalization in the leech are reviewed in section 1.3. The last section of this chapter describes the specific aims of my Ph.D. thesis.

1.1 The central nervous system of the leech

1.1.1 Structure of the central nervous system of the leech

Leeches are segmental worms belonging to the class of Hirudinea, which includes about 650 species, related to the class of the earthworms (Oligochaeta). Unlike earthworms,

leeches have a fixed number of segments, 32, plus a non-segmental prostomium. The species *Hirudo medicinalis*, also called European medicinal leech, on which all the experiments of my thesis have been performed, will be described here.

The leech is a segmented animal: its body is composed of a fixed number of similar segments which are linked and coordinated one to another. The adult leech *Hirudo medicinalis* consists of 4 partially fused segments in the head region, 21 segments along the body and 7 modified segments in the posterior region, forming the tail (Muller et al., 1981). The outer surface of the leech consists of 102 annuli (rings), each segment consisting of 5 annuli except at the head and the tail (see **Fig.1.1**).

The structure of the CNS reflects this segmentation. The total number of neurons is about 15.000-20.000, and many of these neurons are organised in a repetitive pattern in the segmental ganglia. As illustrated in **Fig. 1.1A**, the leech CNS lies within the ventral blood sinus and consists of a ventral nerve cord composed of a chain of segmental ganglia linked one to another by bundles of axons (connectives). The 21 segmental ganglia (G1-G21) are numbered sequentially from the anterior to the posterior region and are almost identical, except for G5 and G6, which innervate the sexual organs. The first 4 ganglia in the head region (H1-H4) are fused and modified to form the brain, while the last 7 ganglia (T1-T7) are fused in the specialized tail brain.

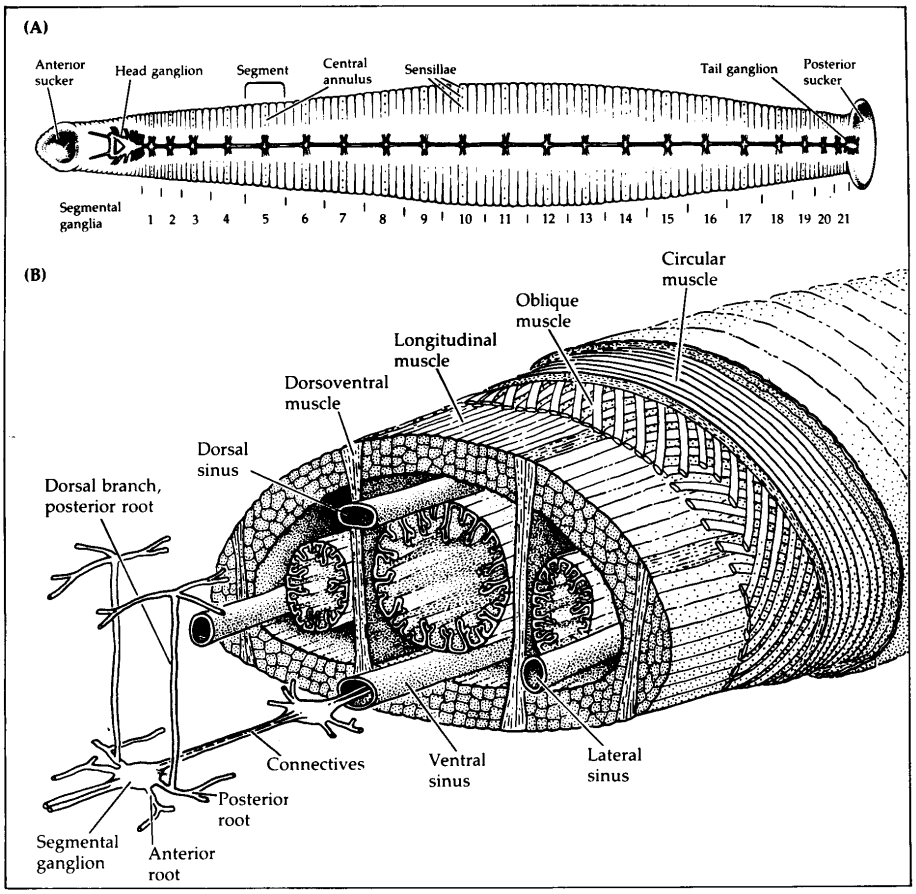

Figure 1.1 The leech central nervous system. A: Schematic diagram of the leech showing the segmentation and the two specialized regions of anterior and posterior suckers. The CNS consists of a ventral nerve cord composed of a chain of 21 segmental ganglia and two more specialized head and tail ganglia, linked one to the other by bundles of axons (connectives). Segments are indicated, composed of five annuli, the central one of which contains sensillae, specific sensory organs. B: Cross-section of the leech showing its anatomy. The body wall is made-up of three layers of muscles (circular, oblique and longitudinal), dorso-ventral muscle fibers run from the dorsal to the ventral side of the animal. The nerve cord lies in the ventral part of the body and it is surrounded by the ventral blood sinus. Ganglia innervate the body wall through the anterior and posterior roots. The posterior root bifurcates near the ganglion and the dorsal branch crosses the body ventro-dorsally to innervate the dorsal region. The other roots innervate lateral and ventral regions.

(From: Nicholls et al., 1992)

The leech performs its spectrum of behaviours using four major types of muscles (**Fig.1.1B**). From the inner to the outer part of the body wall, three layers of muscle fibers are located: longitudinal, oblique and circular, respectively. These muscles form the major portion of the body wall. Longitudinal muscle contraction shortens the animal, while circular muscle contraction elongates it. The oblique muscles are responsible for twist movements of the body. Dorso-ventral muscle fibbers run between the dorsal and ventral parts of the body wall and their contraction flattens the animal. A further kind of muscles, the annulus erectors (not shown in **Fig.1.1B**) are composed of short longitudinal fibers that traverse a single annulus just bellow the epidermis. Contraction of the erectors raises the annuli, forming a series of sharp ridges on the epidermis.

1.1.2 The segmental ganglion

The leech segmental ganglion is bilaterally symmetrical, about 0.6 mm in diametar. It contains the cell bodies of about 200 bilateral pairs of neurons, as well as a few unpaired neurons (Macagno, 1981). Its aspect and structure are conserved from segment to segment and from animal to animal; indeed the same neurons can be identified in each ganglion by their positions, dimensions and functions. All neurones in leech ganglia are monopolar. The cell bodies are contained in six separated regions (packets): a pair of anterolateral packets, a pair of posterolateral packets and a pair of ventromedial packets, each enveloped by one giant glial cell. The connections of the cells are made in the central neuropil, a special region in which synapses are arranged, surrounded by two giant glial cells (Muller et al., 1981); two other glial cells form the nuclei of the connective nerves.

The parallel pair of connectives extend anteriorly and posteriorly from the ganglion (there is actually a third, small, medial connective called Faivre`s nerve). Each of the segmental ganglia innervates a well defined segment of the body wall by way of two pairs of nerves (roots) arising symmetrically from the left and right sides (**Fig 1.1B**). The four roots are defined as anterior and posterior, left and right. The two posterior roots bifurcate near the ganglion, each one giving rise to two branches called posterior-posterior nerves (PP) and dorsal posterior nerve (DP). Through these nerves the ganglion innervates the whole segment. DP nerves innervate the dorsal part of the animal, while the anterior and PP nerves innervate the territory corresponding to the lateral and ventral part of the animal.

The neurons in the leech CNS are relative large (10-60 μm). They can be classified in three categories: sensory neurons, interneurons and motoneurons. Sensory neurons directly translate a physical input coming from the environment into electrical signals, and thereby transduce a physical quantity like pressure, light, concentration into a change of electrical properties (Nicholls and Baylor, 1968; Blackshaw, 1981; Blackshaw et al., 1982; Peterson, 1983; Peterson, 1984; Blackshaw, 1993); sensory neurons also send axons through the connectives. The category of interneurons comprises all neurons whose arborisation does not exit the CNS but can run to neighboring ganglia through the connectives. Motoneurons are responsible for the excitation or the inhibition of muscles (Stuart, 1970; Mason and Kristan, 1982). Motoneurons and sensory neurons project from the ganglion to the periphery through the roots.

The neuronal cell bodies in the ganglion are located on the dorsal and the ventral surfaces. The cell bodies of all mechanosensory neurons lie in the ventral side, while those of motoneurons mainly lie in the dorsal side, with few exceptions (see **Fig.1.2** and **Fig.1.6**).

1.1.3 Propeties of mechanosensory neurons with the focus on morphology

The identification of cells responsive to mechanical stimulation was carried out by Nicholls and Baylor (1968), who found three kinds of neurons responding to three different mechanosensory modalities (see **Fig.1.2**) In each hemiganglion are three T (touch) cells, which respond to light mechanical stimulus applied to the skin, two P (pressure) cells, which respond to stronger stimuli, and two N (nociceptive) cells, which respond to damaging stimulation of the skin, with a threshold more than three times higher than the P cells (Nicholls and Baylor, 1968; Blackshaw et al., 1982). Studies have demonstrated that N cells also exhibit functional properties similar to those of polymodal nociceptive neurons in mammals (Nicholls and Baylor, 1968; Pastor et al., 1996), i.e. they are not simple mechanosensory cells but respond to different sensory modalities of noxious stimulus like high temperature and irritant chemical substances. The intracellular recordings performed from the mechanosensory neurons cell bodies reveal APs with an amplitude larger than 50 mV (Nicholls and Baylor, 1968).

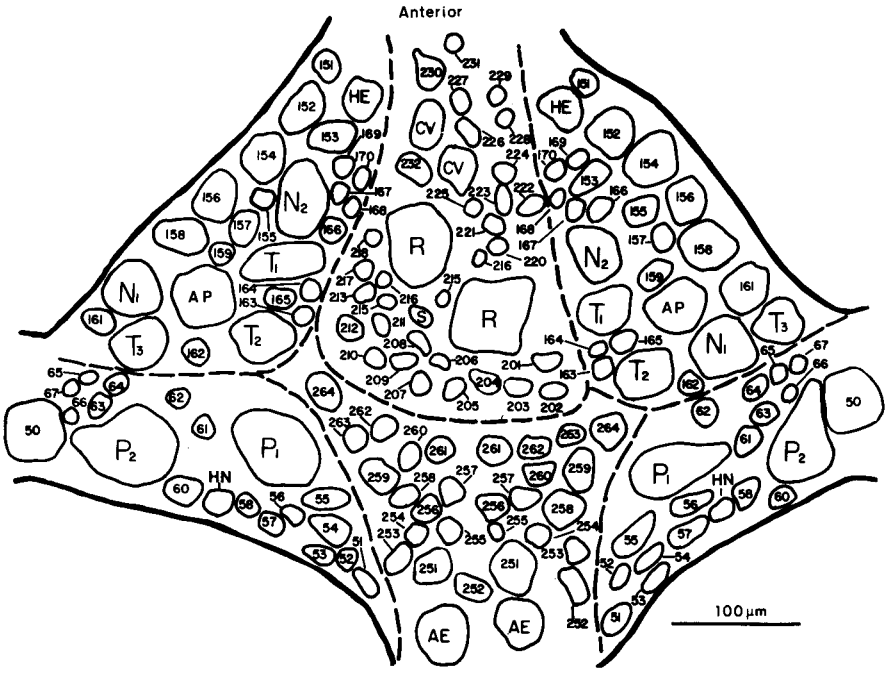

Figure1.2 Cell body map of the ventral aspect of a midbody segmental ganglion of *H.medicinalis*, showing the positions of the different kinds of mechanosensory cells (T, P and N), Anterior Pagoda (AP) and Annulus Erector (AE) motoneuron cells. *(From: Muller et al., 1981)*

Mechanosensory neurons are characterised by a main process arising from the cell body that gives rise to several (primary) branches that leave the ganglion on the ipsilateral side by the roots and connectives (see **Fig.1.3**). Branches that enter the roots are known from physiological studies to innervate the skin and body wall while those in the connectives reach adjacent ganglia (Baylor and Nicholls, 1969; Nicholls and Baylor, 1968; Stuart, 1970) to innervate the roots of adjacent ganglia. The finer (secondary) processes with varicosities arise from the primary branches and the main process and extend in each ganglion into the region called neuropil, the site in which synapses between neurons are concentrated. Varicosities were shown by Muller and McMahan, 1976, to be the locations of chemical synaptic sites, both pre- and postsynaptic, in these cells.

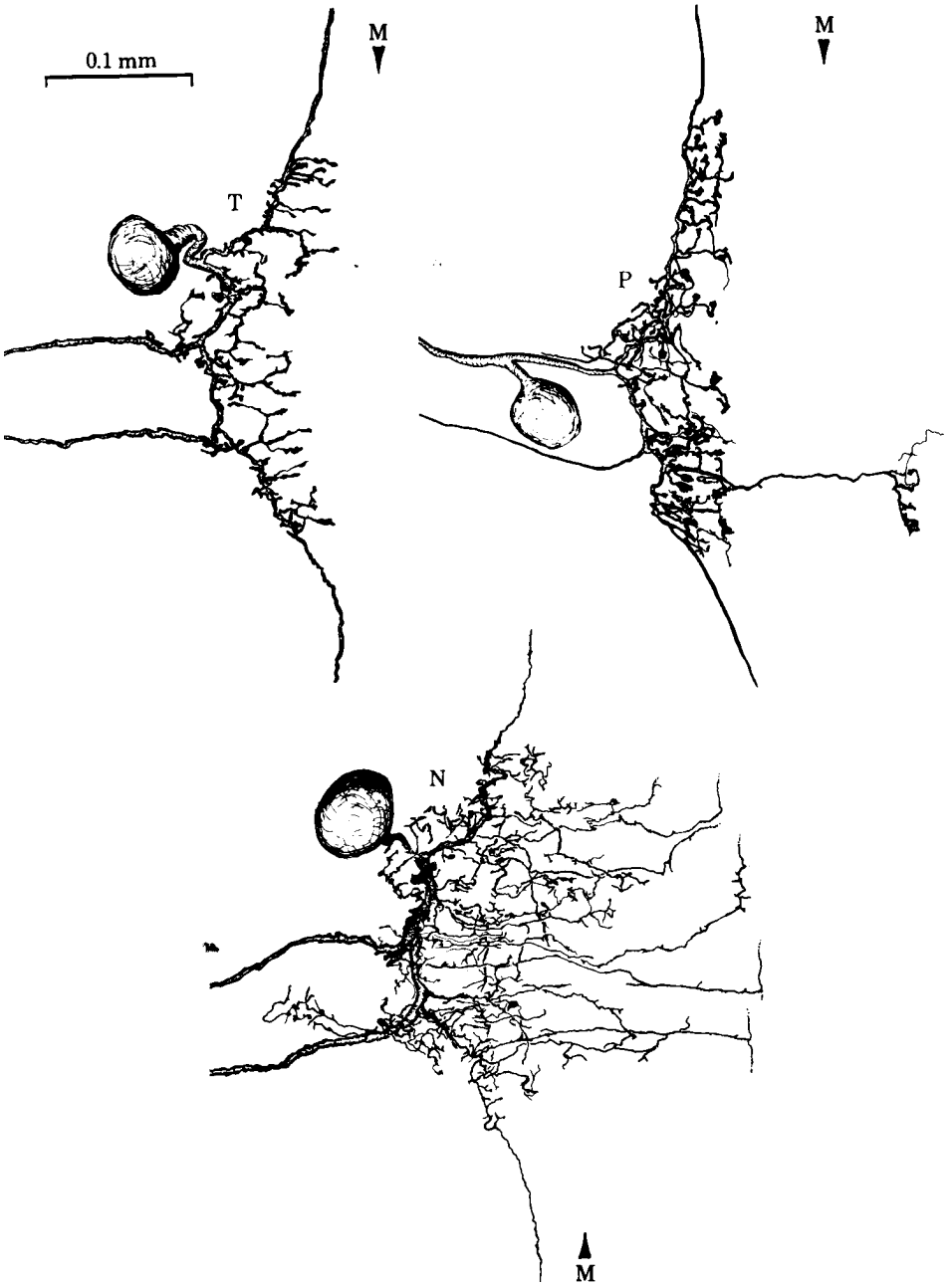

Figure 1.3 Secondary processes of touch (T), pressure (P) and nociceptive (N) cells arise from the main process and its primary branches: most are directed medially. The distribution of processes and the branching pattern characterises each of the three cell types. Drawn with camera lucida from cells injected with HRP and reacted with benzidine. M, midline. *(From: Muller and McMahan, 1976)*

The anatomical organisation of axon branches reflects the results obtained for the receptive fields (Muller and Mcmahan, 1976; Blackshaw, 1981; Blackshaw et al., 1982). The mechanosensory cells in each ganglion innervate a well defined territory of the skin in the corresponding segment (Nicholls and Baylor, 1968; Blackshaw, 1981; Blackshaw et al., 1982). For example the three T cells respond respectively to stimulation of the ventral (Tv), lateral (Tl) and dorsal (Td) region of the segment. Similarly, the two P cells respond to ventral (Pv) or to dorsal (Pd) pressure stimuli. For the two N cells (Nm, Nl) the receptive fields in the same ganglion are approximately coincident and span the entire hemisegment from dorsal to ventral midline. From the study of the anatomy and the physiology of mechanosensory neurons, their receptive fields appear to be composed of several contiguous sub-fields (see **Fig.1.4**) innervated by separate branches of the same cell (Nicholls and Baylor, 1968) passing through the roots of their ganglion and those of adjacent ganglia (Yau, 1976). On the other hand, by comparing the extent of receptive fields of different cells responsible for the same sensory modality in a single ganglion or in two adjacent ones, a considerable overlapping between receptive fields has been observed, as shown in **Fig 1.4** (Nicholls and Baylor, 1968).

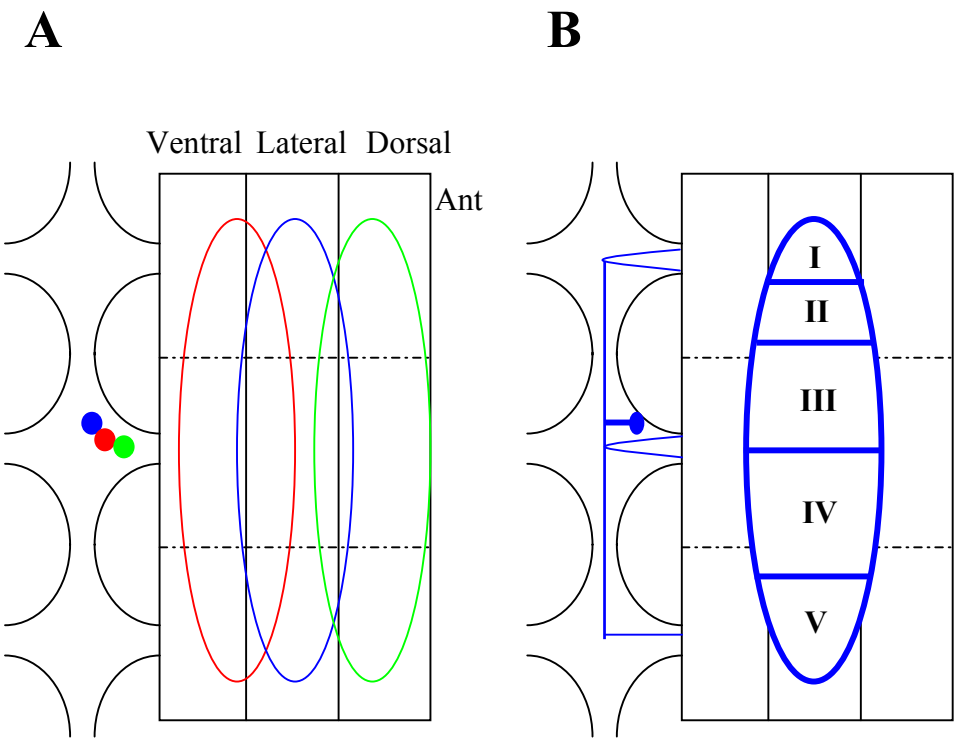

Figure 1.4 Organization of the receptive fields. A: Boundaries of the receptive fields of three T cells in the same ganglion overlap. The cells are drawn in the same color as their receptive fields. T_v is represented in red, T_l in blue, T_d in green. B: Adjacent subfields (I II III IV V) of a T_l cell, innervated by separated branches, do not overlap

The synaptic regions of all the mechanosensory neurons are situated mainly on secondary processes. Each synaptic region contacts a multiplicity of postsynaptic processes and each synaptic region receives one or more presynaptic axon terminals (Muller and McMahan, 1976). Examples where inputs directly contact regions of output, as found in the leech, occur in several regions of vertebrate CNS, including the spinal cord, retina and thalamus (Dowling, 1970; Lieberman and Webster, 1974) and in other invertebrates (Gray and Young, 1964; Dowling and Chappell, 1972).

Each mechanosensory neuron type has a distinctive mode of action potential firing and action potential shape. The traces in **Fig.1.5** show the response of the cell types to depolarising current pulses. The impulses in the cell body of T cells are always similar but are smaller and briefer than those of P or N cells; N cells are distinguished by their large and long-duration afterhyperpolarisation. During maintained pressure, the T cell is rapidly adapting and usually ceases within a fraction of a second, the P cell discharge is slowly adapting and lasts 20 sec or more. N cells are slowly adapting and often continue to fire after the stimulus has been removed. The frequency of firing of all three mechanosensory neuron types is graded with the extent and degree of the indentation while each cell type needs different intensity of mechanical stimuli in order to fire, which is expressed in the name of the cell type. The amplitude of the action potential is more than 50 mV; mechanosensory neurons have excitable somata.

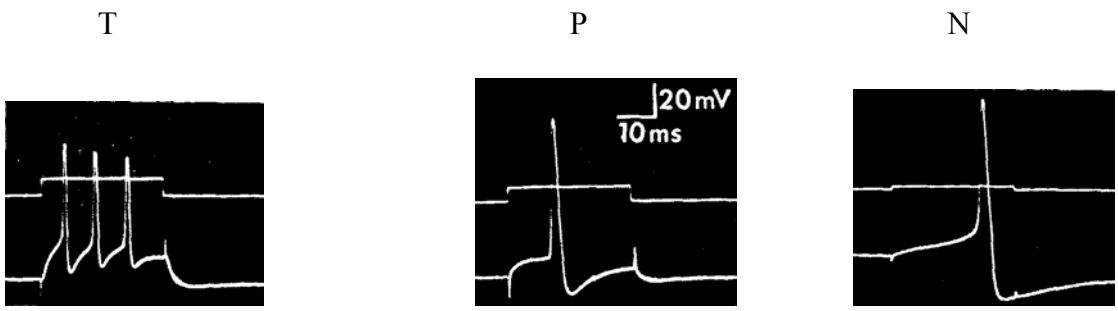

Figure 1.5 The intracellular recording of T, P and N action potentials elicited by passing depolarising current through the microelectrode *(From: Nicholls and Baylor, 1968)*

1.1.4 Properties of motoneurons with the focus on morphology

In each hemiganglion there are 21 excitatory and 7 inhibitory identified motoneurons (Nicholls and Baylor, 1968; Stuart, 1970; Ort et al., 1974; Stent et al., 1978; Mason and Kristan, 1982; Norris and Calabrese, 1987; Baader, 1997). When the ganglion is observed in transmitted light, 25 motoneurons are visible on the dorsal side and 3 are visible on the ventral side (see **Fig.1.2** and **Fig.1.6**). All motoneurons are present as pairs on the left and right hemiganglia.

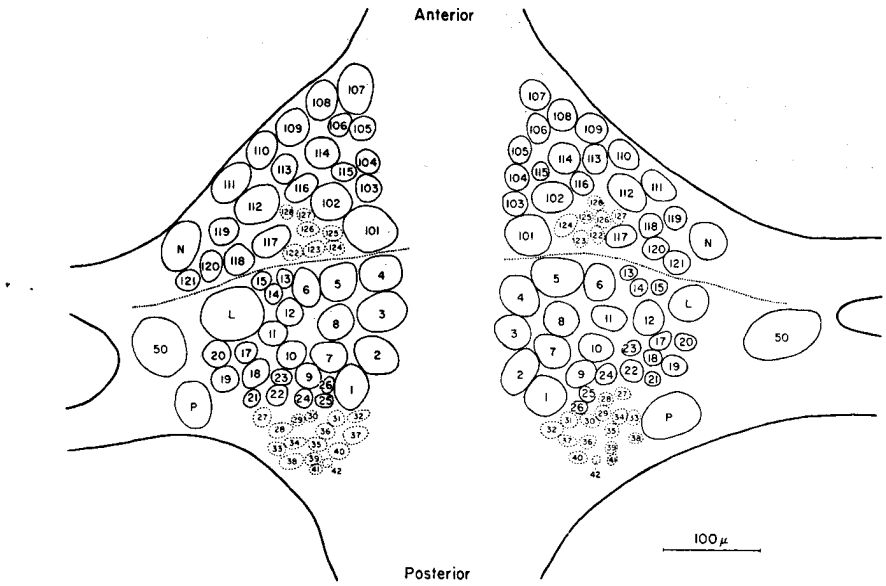

Figure 1.6 Cell body map of the dorsal aspect of a midbody segmental ganglion of *H.medicinalis*. *(From: Muller et al., 1981)*

With the exception of the Annulus Erector (AE), which erects the skin at the center of the annuli, and the heart excitor (HE), which supplies the lateral heart tubes, they are responsible for leech locomotion and movement. They can be divided into four groups, according to the muscle fibers they innervate: longitudinal, circular, oblique and dorsoventral. With only the exception of cell 4, a ventral longitudinal excitor, and cell 117, a dorsoventral excitor, all motoneurons exit the ganglion via the contralateral roots to innervate the corresponding body wall (Ort et al., 1974). The main process of each motor neuron crosses the midline and bifurcates in the contralateral neuropil, forming two primary branches that enter the roots on that side. Numerous highly branched secondary processes radiate from the main process and its primary branches and extend within the neuropil (see **Fig.1.7** and **Fig.1.8**). The fields of innervation of motoneurons extend longitudinally into adjacent body segments (Blackshaw, 1981) and frequently overlap

with those of neurons supplying the same muscle group. The motoneurons probably innervate muscle fibers by many terminals along their length, as in crustacea (Stuart, 1970).

Unlike in the mechanosensory neurons, the soma and the proximal axonal regions of leech motoneurons are unexcitable. The action potentials arise at a site distant from the soma, near the primary bifurcation of the axon (Gu et al., 1991). For this reason, only small action potentials (few mV in amplitude), which are the results of the passive propagation of the action potential from the spike generation to the soma, are visible in intracellular recordings performed from the motoneuron cell bodies (Stuart, 1970).

Motoneurons are postsynaptic and receive input on short branches and spines, which are distributed along both primary and secondary processes (Muller and MacMahan, 1976).

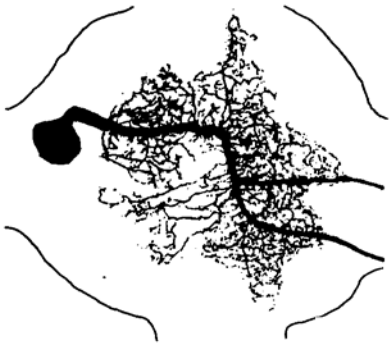

Figure 1.7 Distribution of AP neurone processes within the ganglion. The main process crosses the ganglion and bifurcates to enter the contralateral roots. The outline of the ganglion is indicated by the line drawing. *(From: Wessel et al., 1999)*

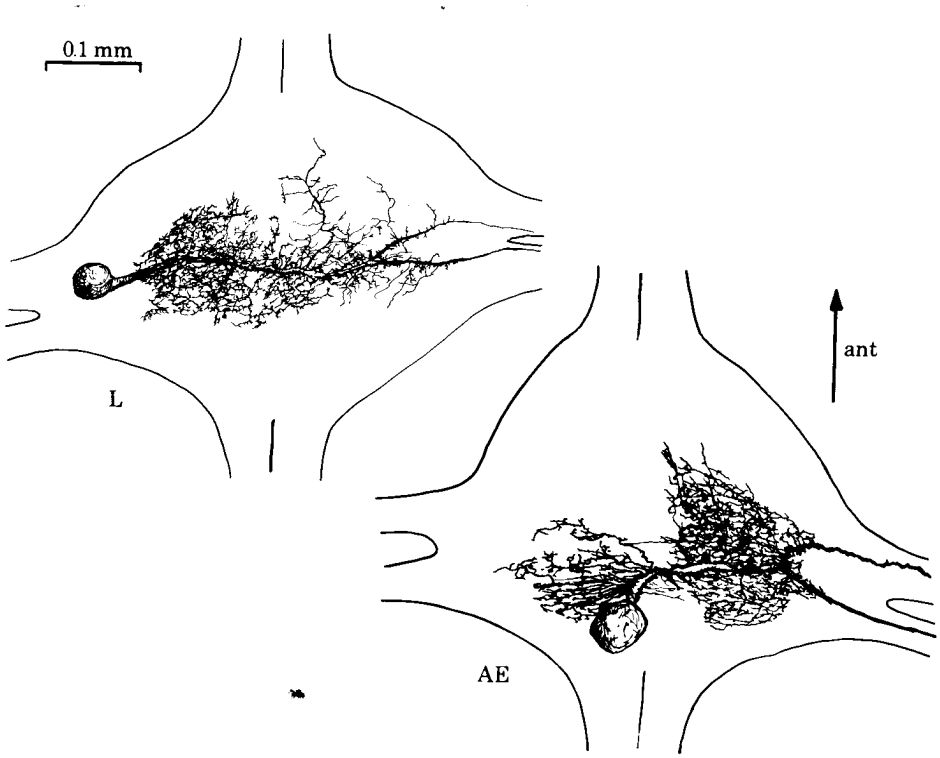

Figure 1.8 Distribution of L and AE motoneurone processes within the ganglion. In both cases the main process crosses the ganglion and bifurcates to enter the contralateral roots. The pattern of secondary process is distinctive and typical for each neurone type. *(From: Muller and McMahan, 1976)*

There is good evidence that the leech longitudinal nerve muscle junction is cholinergic (Gardner and Walker, 1982) and more generally that excitatory motoneurons synthesize, accumulate and release acetylcholine (Norris and Calabrese, 1987). The leech inhibitory motoneurons are thought to be GABAergic (Blackshaw and Nicholls, 1995), since the longitudinal motoneurons take up and synthesise GABA from the precursor glutamate and further, central and peripheral inhibitory synaptic effects are mimicked by GABA(Cline 351-58).

1.2 Functional organisation and calcium dynamics

1.2.1 Functional organisation of the neuron

The primary function of neurons is information transfer. This includes both intracellular signalling, from one part of a neuron to another of the same cell, and intercellular signalling, from one neuron to another or to a muscle cell (Nicholls et al, 2001; Levitan and Kaczmarek, 1997).

The language of intracellular signalling in nerve cells is primarily electrical. There is a voltage difference across the plasma membrane, and information is carried from one part of the cell to another in the form of action potentials, large and rapidly reversible fluctuations in the membrane potential that propagate along the axon. The electrical activity of nerve cells depends on the movement of the charge, carried by small inorganic ions, across channels in the plasma membrane. Electrical signalling is based on the opening of the voltage-sensitive ion channels, which are the class of specialised membrane proteins that span the plasma membrane forming hydrophilic pores through which ions flow from one side of the membrane to the other down their electrochemical gradient. Pumps and carriers play only a supporting role in electrical signalling in most nerve cells.

The firing pattern of a neuron can be seen as a play of interactions among the currents generated by the different kinds of ion channels in its membrane. The activities of the sodium and potassium channels responsible for the axonal action potential are dependent on voltage. Voltage clamp studies have provided a detailed understanding of the sequence of changes in channel activity that give rise to action potentials.

1.2.2 Calcium dynamics in neurons

Calcium ions may enter the cytosol through voltage-gated channels (for review, see McCleskey, 1994; Dolphin, 1996). This may contribute to the modulation of electrical excitation and propagation of APs, and to different modes of synaptic and nonsynaptic processes. Calcium channels are found in all excitable cells. They play an important electrical and transducing role.

Most neurons exhibit a substantial voltage-dependent calcium current, which in some cases is responsible for much of the depolarisation during the rising phase of the action potential (Duch and Levin, 2000). Calcium channels are distributed in a non-uniform manner over the surfaces of neurons. For example, presynaptic motor nerve terminals (Katz and Miledi, 1965; Augustine et al.1989; Stanley and Goping 1991; Cohen et al. 1991) and dendrites of cerebellar Purkinje cells (Ross and Werman 1986; Hockberger et al.1989) show higher densities than their axons or cell bodies. Little is known about the mechanisms that determine how calcium channels are placed in the neuronal membrane.

In dendritic processes of neurons, calcium channels contribute electrically to summing and spreading synaptic inputs that will drive the action-potential encoding region of the proximal axon (Llinas and Sugimori, 1980; Llinas and Yarom, 1981). In nerve cell bodies of molluscs, annelids, arthropods, amphibians, birds and mammals, it was demonstrated that calcium channels coexist with sodium channels and that make a partial contribution to electrical excitability (see Hille, 1992, and references therein). Ca^{2+} transients induced by single APs have been studied in detail in mammalian pyramidal neurons, showing Ca^{2+} signals in dendrites, and in particular in presynaptic terminals (Schiller et al, 1995; Beier and Barish, 2000). Axonal calcium signalling

due to single APs has been studied in rat cerebellar Purkinje neurons, showing only small calcium transients in the axon, while calcium influx of much higher amplitude was found in the dendrites and the submembrane region of the cell body (Eilers et al. 1995; Callewaert et al,. 1996). Less is known about the spatial distribution of AP induced calcium transients in invertebrate neurons. One of the first studies showing calcium transients accompanying APs was performed in the cell bodies of Aplysia neurons (Gorman and Thomas, 1978).

Calcium channels are of particular interest because calcium is far more than simply a charge carrier across the plasma membrane. The role of calcium in contributing to action potentials and other aspects of neural electrical activity can be secondary to the intracellular messenger action of calcium. Calcium channels are the only link to transduce depolarisation into all the nonelectrical activities that are controlled by excitation. Without calcium channels our nervous system would have no outputs (Hille, 1992). Calcium that enters the cell interacts with calcium binding proteins to regulate a variety of intracellular enzymes. Furthermore, intracellular calcium ion regulates the gating of several types of ion channel, and can even feed back and participate in inactivation of one of its own channels. In addition, an essential characteristic of neuronal signalling, the release of chemical neurotransmitters at synapses, is controlled directly by intracellular calcium. In this sense calcium can be thought of as the transducer of an electrical signal, depolarisation, into chemical signals inside the cell.

Calcium channels are found at high density only in nerve terminals close to release sites. Perfectly selective blocking agents for calcium channels are rare and substitution of other cations for external calcium alters the gating characteristics of almost all known channels.

In a resting cell the cytoplasmic free calcium level is held extremely low. The normal resting Ca^{2+} concentration lies in the range 20 to 300 nm in living cells. Internal K^{+} ions are 6 to

10 times more concentrated than internal Ca^{2+} ions. Quite in contrast to the situation with Na^{+} or K^{+} ions, the normal Ca^{2+} concentration is so low that it may be increased dramatically during a single depolarising response in a cell with Ca-channels.

Multiple channel types can coexist in the same cell (Kostyuk 1990; Tsien and Tsien, 1990). A striking difference between classes of calcium channels is their sensitivity to depolarisation. LVA- low voltage activated calcium channels activate with small depolarisation and HVA-high voltage activated calcium channels require high depolarisation.

Since 1973, when it was found that calcium influenced a potassium conductance in leech neurons (Jansen and Nicholls 635-65), and a year later when it was discovered that calcium ions activate a class of K^{+} channels when injected into molluscan neurons, calcium dependent K^{+} channels have been found in many animal preparations. Evidence for Ca^{2+}-activated K^{+} channels in dendrites has been found in rat Purkinje neurons (Khodakhan and Ogden, 1993), in rat hipocampal pyramidal neurons (Andreasen and Lambert, 1995; Sah and Bekkers, 1996) and in rat neocortical pyramidal neurons (Schwindt and Crill, 1997).

1.3 Calcium dynamics in leech neurons

An early study of calcium distribution in identified leech neurons in culture by using the optical recording with a photodiode array was done by Ross et al. 1987, in which calcium transients were recorded from the soma of all mechanosensory neurons and Retzius cells.

Different size and kinetics of the AP-induced Ca transients in the axons and dendrites of the leech Retzius neuron are described by Beck et al., 2001. By using the voltage-sensitive dyes,

Fromherz and Vetter (1991) found APs pervaded the neurites of cultured Retzius cell without significant change of amplitude but with enhanced pulse width.

The Anterior Pagoda neurons express Ca-activated K conductances that are present in the neurites and that regulate electrical signal propagation (Wessel et al. 1999). There is preliminary evidence for Ca-activated K channels in somatic membrane patches of the Anterior Pagoda neuron (Pellegrini et al. 1989) as well as in somata of other leech neurons (Jansen and Nicholls, 1973). Evidence for calcium current in the Anterior Pagoda cell has been reported (Stewart et al., 1989). The spike initiation site is far from the soma in Anterior Pagoda neurons (Melinek and Muller, 1996).

The primary axon bifurcation of the Annulus Erector motoneuron is the site of integration of synaptic potentials that spread passively from both sides of the ganglion (Gu et al., 1991).

1.4 Aim of the work

We have studied the active properties of leech mechanosensory neurons and motoneurons by using a combination of calcium imaging and intracellular recordings. The specific question addressed in the present study was whether these neurons express a high density of calcium channels and whether the density of the channels is different in specific regions of the neuronal arborisation. We found that for mechanosensory neurons the density of calcium channels appears to be the same in the cell body and in processes, while in motoneurons the density of calcium channels appears to be much higher in the region of the first major bifurcation and distally from it than in the region of the cell body. The results obtained by studying the mechanosensory

neurons are presented in Chapter 3, and in Chapter 4 are presented the results obtained by studying motoneurons.

2 Materials and methods

The experiments described in this thesis were performed in the leech CNS. In this chapter the experimental procedures and methods of analysis are explained.

2.1 Animals, preparations and solutions

2.1.1 Animals and preparations

Specimens of *Hirudo medicinalis* were obtain from a commercial supplier (Ricarimpex, Eysines, France) and kept at 5 ^{o}C in tap water dechlorinated by aeration for 24 hours. The leeches were dissected under a dissecting microscope.

An isolated ganglion of the leech was used. A single midbody ganglion was dissected from the leech CNS by making an incision along the dorsal midline of the leech body. It was then pinned through the connectives on a Sylgard-coated dish. Having a well-fixed ganglion is important both for intracellular penetration and optical recording; even the small mechanical movements can disturb optical recording. In experiments in which the cells were stimulated with the extracellular electrodes through the roots, the ganglion was pinned through the connectives and the other pair of roots. In experiments in which cells were stimulated with the intracellular electrodes, the ganglion was pinned through the connectives and both pairs of roots. The connective tissue sheath over the neuronal soma was occasionally removed with fine tweezers in

order to facilitate intracellular penetration and optical recording. Since mechanosensory neurons are visible from the ventral side of the ganglion (see **Fig.1.2**), ventral side up configuration was used for impaling and stimulating mechanosensory neurons in order to evoke action potentials in them and record optically from them. On the other hand, since most motoneurons are contained in the dorsal side of the ganglion (see **Fig.1.6**), dorsal side up configuration was used for impaling and stimulating motoneurons. Sensory neurons and motoneurons were identified by the size and location of their cell bodies and, during intracellular recording, by their characteristic firing patterns and impulse size and shape (Nichols and Baylor, 1968; Stuart, 1970).

2.1.2 Solutions

Preparations were kept in a Sylgard-coated dish at room temperature (20-24 ^{o}C). During dissection and during experiments, the preparations were bathed in a Ringer solution with the following composition in mM: 115 NaCl, 1.8 CaCl2, 4 KCl, 12 glucose, and 10mM Tris maleate buffered to pH 7.4 with NaOH (Muller et al., 1981).

2.2 Electrophysiology

2.2.1 Intracellular recordings

The electrical activity of neurons was monitored by intracellular recordings (Muller et al., 1981). Intracellular recordings from the soma of selected neurons were obtained by impaling

those neurons with sharp electrodes. The electrodes were pulled (P-97 puller, Sutter Instruments) using thin glass capillaries (TW 1B100F-4, WPI). Electrodes had a resistance between 15 and 50 MΩ. Potassium acetate 4.0 M solution was used to fill the electrodes (Muller et al., 1981). The electrode holders, including head stage, were mounted on micromanipulators (Narishige, Japan). The intracellular recordings were performed using an Axoclamp-2b amplifier (Axon Instruments, Foster City, CA) and RedShirtImaging software.

The sensory input was mimicked by evoking action potentials in mechanosensory neurons by passing depolarising current pulses through the electrode into the cell bodies. Action potentials were evoked similarly in the motoneurons. Stimulation was controlled by the RedShirtImaging software through the AxoClamp 2B.

2.2.2 Extracellular recordings

Suction pipettes were used for extracellular stimulation of nerve roots emerging from the segmental ganglion and to analyze calcium dynamics initiated by the stimulation of distal processes (see **Fig.4.4**). The pipettes were obtained by pulling (P-97 Flaming/Brown micaropipette puller, Sutter Instruments) thick walled glass capillaries (TW 100-4, WPI). After pulling, the capillaries were cut on the tip and shaped with the microforge, in order to match the section diameter of the root we had decided to stimulate. The pipets were positioned near roots using micromanipulators (Narishige, Japan). Roots were stimulated by applying a current pulse of 0.2 s with an intensity able to evoke a brief discharge of at least three APs. The posterior or the anterior root was stimulated antidromically while a suction electrode on the other root was used for recording. Electrodes were connected to the RedShirtImaging interface through a

stimulator (Axon Instruments, Isolator-10 stimulus isolation unit) and the stimulation was controlled by the RedShirtImaging software.

Extracellular voltage signals were recorded using a homemade 8-channel amplifier, whose head-stage had a bandwidth of 200-2000 Hz and a gain of 10^3. The second stage of amplification was contained in the rack mounted box that had a gain ranging from 1 to 50. The signal produced by the action potentials, recorded by the suction electrodes from the roots, ranged between 15 and 500 μV. The standard deviation of the noise was about 10μV.

Both intracellular and extracellular recordings were digitised at 10 kHz and stored on a personal computer using the acquisition board Digidata 1200B and the software Clampex 8 (Axon Instruments) (see **Fig 2.1**).

2.3 Optical recordings

To decide on which method to use for optically recording from single living neurons it is necessary to define exactly what one wants to record and how one wants to do it. Specifically, deciding what to record involves determining a parameter of interest (e.g., membrane potential or ion concentration), the nature of the information required (e.g., qualitative or quantitative) and the optical indicator best suited to making these measurements. Likewise, deciding how to record these signals involves consideration of recording methodologies (e.g., imaging), experimental procedures (e.g., loading and staining protocols) and data processing techniques (i.e., signal processing and analysis). o

2.3.1 Dye characteristics, preparation and loading

The long-wavelength calcium indicators Oregon Green and Calcium Green are visible light excitable probes. Upon binding to calcium, these indicators exhibit an increase in fluorescence emission intensity (F_{Ca}/F_{free}~14) with little shift in wavelength so they belong to a class of qualitative indicators which simply change their brightness in proportion to bound calcium, in contrast to quantative, ratiometric indicators which commonly undergo calcium-dependent spectral shifts. The major difference between Oregon and Calcium Green is that both the fluorescence excitation and emission maxima of the Oregon Green 488 BAPTA indicator are shorter by ~10nm. The extinction coefficient for Oregon Green 488 BAPTA-1 absorption at 488 nm is ~93% of its maximal value, whereas for Calcium Green-1 is only about ~ 45% of maximum.

For intracellular injection, 3 mM of the dye Oregon Green (Oregon Green 488 BAPTA-1, hexapotassium salt, cell impermeant, Molecular probes) was dissolved in 30 mM potasium acetate. In some experiments 300 μM Calcium Green (Calcium Green-1, hexapotassium salt, cell impermeant, Molecular probes) was dissolved in distilled H_2O. These solutions are stable and can be stored at 4 ^oC for several weeks. Oregon Green and Calcium Green have dissociation constants, Kd, for Ca^{2+}, in the absence of Mg^{2+}, of 170 nm and 190 nm respectively, but Oregon Green is more efficiently excited by a 488 nm spectral line than Calcium Green. As a consequence, with a similar dye loading, a larger emitted fluorescence is obtained by using Oregon Green. Before filling the electrodes, dye solution is put on a vortexer and ultrasonic cleaner in order to mix the solution and break the aggregates. The dye was pressure injected with intracellular electrodes into leech neurons. A continuous pressure varying from 5 to 20 psig was

applied to the microelectrode using a pressure injector system (PM2000B 4-Channel MicroData Instrument, Inc.). The dye injection time, and the amount of dye injected was reduced to a minimum that still allowed us to see cell processes. Dye was injected for approximately 5 minutes. After loading the neuron with dye, the ganglion was left in darkness at room temperature for two or three hours before making optical recordings. This allowed spread of the dye into the neural processes. Pharmacological effects impose limitations when using too much dye. It is not always possible to increase the amount of dye in distal processes by putting more dye in the soma because of damage. The absence of large pharmacological effects is evident from the fact that electrically recorded action potentials were essentially unchanged after staining.

Photobleaching is the irreversible destruction of the excited fluorophore. To use lower excitation intensity, detection sensitivity must be maximized by low-light detection devices such as CCD cameras, as well as by high numerical aperture objectives and the widest bandpass emission filters.

2.3.2 Optical recording of calcium transients

Optical recording of membrane potential transients by using Ca-sensitive dyes is an indirect measurement. The quantity that is being measured directly, by photodiodes, is light intensity. Qualitative optical measurements reflect changes in calcium without reference to resting levels or the absolute size of these changes. This kind of change is usually depicted as the change in fluorescence normalized by the overall mean fluorescence, $\Delta F/F$.

Fluorescence is the result of a three-stage process that occurs in molecules called fluorophores or fluorescent dyes. The first stage is excitation. A photon of energy $h\nu_{ex}$. supplied by a light source, gets absorbed by the fluorophore, creating an excited state that exists for a short time during which the fluorophore undergoes conformational changes. An excited state is the second stage. The third stage is fluorescence emission when a photon of energy $h\nu_{em}$ is emitted, returning the fluorophore to its ground state. Due to energy dissipation during the excited-state lifetime, the energy of this photon is lower, and therefore of longer wavelengths, than the excitation photon. In fluorescent measurements, most of the fluorescent dye comes from the stained cell, regardless of the size of the image relative to the size of the detector, but, background fluorescence can become dominant when the process is extremely small or poorly stained. As only one cell is stained in the ganglion, the source of the signal is certain, and signals can safely be attributed to potential transients in the specific regions of the neuron.

An advantage of calcium indicators is their excellent signal-to-noise ratio. This signal-to-noise ratio is partially owing to the excellent calcium indicators available, but is also related to the large changes in intracellular calcium concentration that occur following an action potential. The intracellular calcium concentration can change by one to two orders of magnitude, in contrast to other intracellular ions, whose concentrations change far less. Hence fluorescent indicators for sodium ions offer a more direct measure of propagation of APs, the relatively small sodium concentration changes that occur lead to the small fluorescent change. A second advantage of calcium indicators is that their toxicity is minimal so that they have little effect on dendritic function. One exception is the effect on the calcium-activated potassium channels that play a role on suppressing action potential initiation or in repolarisation. Calcium dyes bind calcium so there is a low concentration of free calcium even if the calcium is raised. This means

that calcium dyes can damage the function of the cell if it depends on the concentration of the calcium, for example AP propagation can be disturbed if it depends on the Ca^{2+}-dependent K^{+} channels.

A disadvantage of calcium indicators is their poor temporal resolution compared to electrophysiological and voltage-sensitive dye techniques. The factor limiting the temporal resolution is the binding of calcium to fluorescent indicator. Following an action potential, equilibration of free and indicator-bound calcium may continue over several milliseconds (Sabatini and Regehr, 1998).

A second disadvantage of calcium indicators is that they provide no direct measure of depolarisation. Calcium indicators are accordingly used to image the sites of action potential initiation and propagation. Often it is possible to demonstrate that a calcium signal results from active AP propagation if the calcium signal is attenuated when sodium channels are blocked by using TTX. But, changes in calcium channel density or subtype along the length of a dendrite may influence calcium influx, regardless of any change in AP amplitude or halfwidth.

By comparing electrical signals with optically recorded action potentials one can assess how accurately the events are followed. In a typical experiment, the cell was stimulated by passing current through a microelectrode to produce action potentials, while simultaneously recording optical signals from multiple sites on the neuron.

2.3.3 Optics

A stereomicroscope (SMZ-2B, Nikon) was used during the dissection. The preparation was then transferred to an anti-vibration table, where impaling neurons under visual control was

possible in dark field illumination, obtained by mounting a dark field condenser (Leitz Wetzlal) onto the microscope (Fixed stage upright, Olympus). This microscope was also used for imaging.

2.3.4 Imaging

The preparation was placed on the stage of a microscope and the image of the stained cell was projected onto the fast CCD camera. This camera allows fast, multisite optical monitoring of membrane-potential changes. The preparation was illuminated with a halogen lamp (Olympus) or a xenon lamp (Optiquip). The xenon lamp was approximately 10 times brighter than the halogen lamp and was used when it was necessary to analyse calcium dynamics in the fine dendrites. The preparation was illuminated through the objective (40x/0.8 NA, water immersion, LUMPlanFI) and a dichroic mirror was used (U-MSWB filters: exciter filter BP 420-480 nm, barrier BA > 515 nm and dichroic mirror 500 nm). In epifluorescence, both the excitation light and the emitted light pass through the objective, and the intensity reaching the photodetector is proportional to the fourth power of the numerical aperture. Fluorescence emitted by the dye was measured with the fast CCD camera NeuroPlex (RedShirtImaging). The software provided by RedShirtImaging controlled the opening of the shutter at the beginning of the acquisition and its closing at the end of the acquisition and allowed setting the duration of acquisition, the beginning and the duration of stimulation, as the acquisition sampling rate. Images were acquired at a sampling rate of 1 kHz for 2 seconds and the sequence of fluorescence images F(n) was analysed by the same software provided by RedShirtImaging and by the software that we made in the lab. The spatial resolution of the fast CCD camera was 80 x 80.

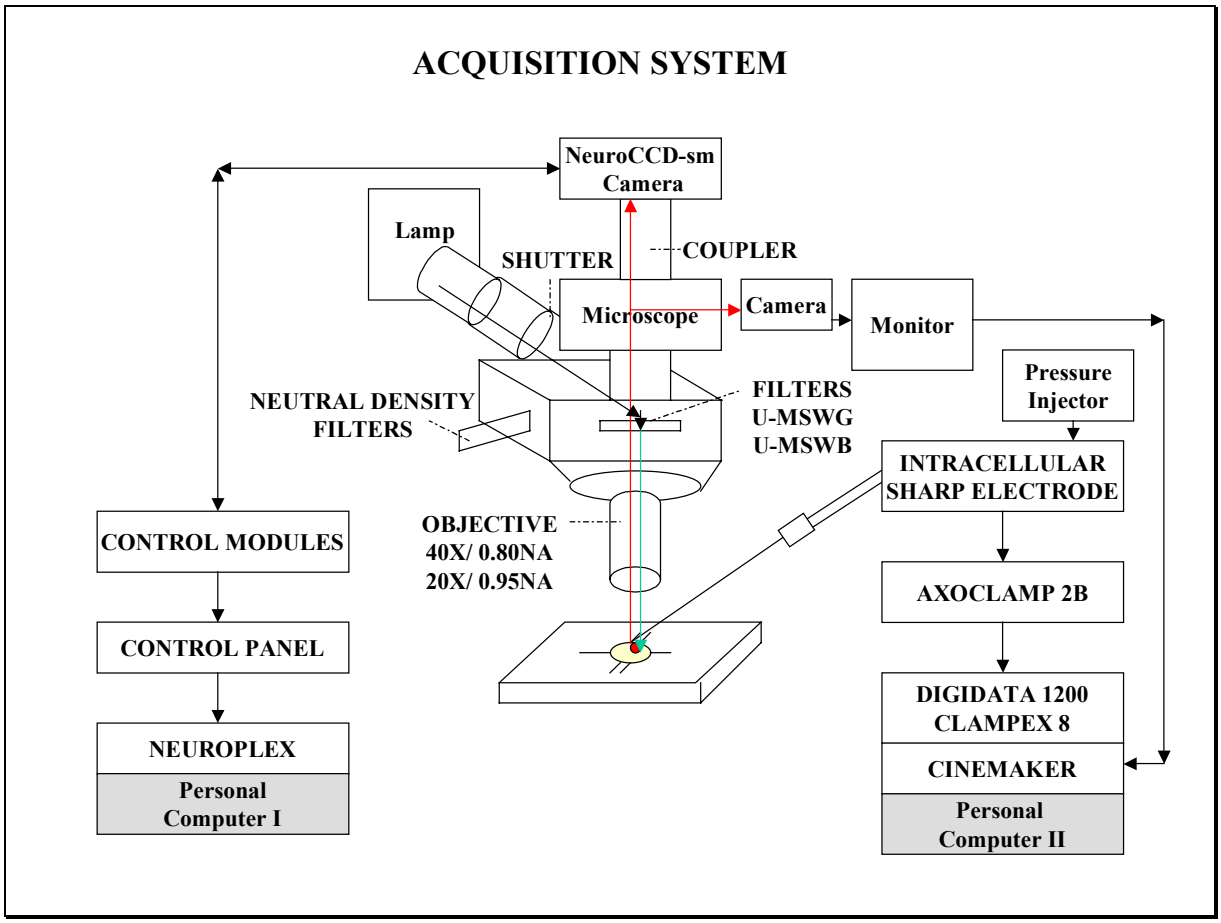

Fig 2.1 Acquisition system

2.4 Data analysis

Fluorescence images F (n) obtained by the fast CCD camera, were averaged from $F(n_1)$ to $F(n_2)$, where $F(n_1)$ corresponded to the image acquired just after shutter opening and $F(n_2)$ corresponded to the image acquired just before stimulation. The averaged image F was used as

the resting fluorescence light intensity (see **Fig.2.2A**). Fractional fluorescence changes ΔF(n)/F were computed from the image sequence F(n) using the following procedure.

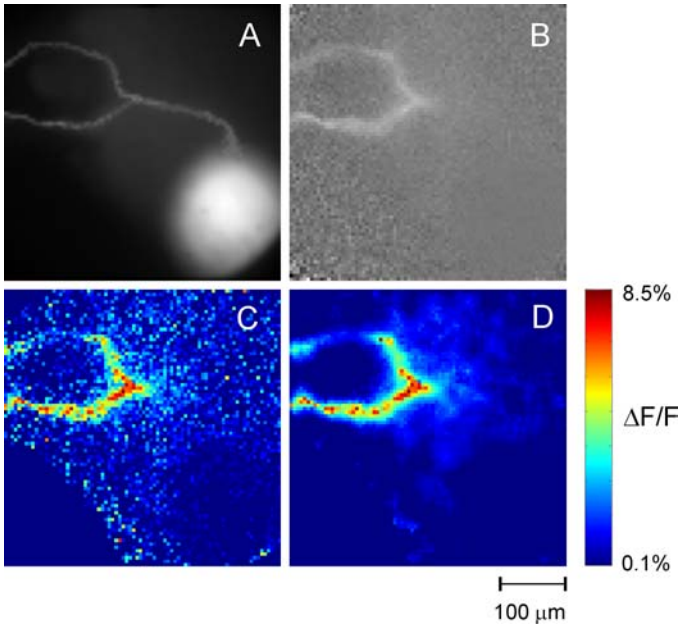

Figure 2.2 Processing of fluorescence images. A: a low resolution (80x80) image of an Annulus Erector motoneuron. B: a low resolution image (80x80) of ΔF/F, i.e. is the optical signal ΔF/F averaged over 2000 images acquired during an individual trial. In this case the cell was stimulated with a depolarising current pulse, which evoked 7 APs. In B white indicates large values of ΔF/F. C and D: unfiltered and filtered images of ΔF/F respectively. In C and D a colour-coded scale was used, with deep red corresponding to a fractional fluorescence of 8.5 %. Deep blue corresponds to a fractional fluorescence change of 0.1% just above the noise level. Th_1=1% Th_2 =3%. See Methods for further details.

The time constant τ of bleaching was computed by fitting with the equation $F_0 e^{-t/\tau}$ the fluorescence observed between shutter aperture and electrical stimulation, where F_0 is the

fluorescence intensity measured immediately after the shutter opens. Typical values of τ varied between 1 and 2 seconds. Corrected fluorescence F*(n) images were obtained as

$F^*(n)= F(n)\ e^{(n-m)\Delta t/\tau}$ where m is the number of the image corresponding to the shutter opening and Δt is the interval between two successive images (Δt is the inverse of the sampling frequency of image acquisition). $\Delta F(n)/\underline{F}= (F^*(n)-\underline{F})/\underline{F}$ was then computed and in order to avoid the noise originating from dividing by small numbers, $\Delta F/F$ was multiplied by a factor equal to $F^2/(F^2+Th_0^2)$. This factor was introduced to eliminate the big values of $\Delta F(n)/F$ which appear on the boarders of the image where F is near to 0. Th_0 is the correction factor which value was determined empirically. A value of Th_0 corresponding to a fluorescence value of 5 was used for Th_0. In order to reduce the noise further an adaptive spatial filtering was also used. The value of $\Delta F/F$ was averaged over the entire image sequence and $\Delta F/F$ was obtained (see **Fig.2.2B**). Pixels with a high value of $\Delta F/F$ are those where the optical signal is significant and relevant. The value of $\Delta F/F$ was spatially filtered in the following way: if $\Delta F/F$ was less than Th_1, $\Delta F/F$ was spatially averaged over a mask of 5x5 pixels, if $Th_1 < \Delta F/F < Th_2$ the mask was 3x3 and if $\Delta F/F$ was greater than Th_2 no spatial filtering was used. **Fig.2.2C and D** compare an unfiltered and filtered image of $\Delta F/F$, when the values of 1% and 3% were used for Th_1 and Th_2 respectively. The resulting image sequence $\Delta F/F$ was viewed with a colour-coded map, where deep red was the highest fluorescence change.

3 Calcium dynamics in mechanosensory neurons

3.1 Results

I used the preparation described in Section 2.1.1 to characterize the calcium dynamics and distribution resulting from action potentials in cell bodies and processes of leech mechanosensory T, P and N neurons. The experimental set-up allowed recording of calcium transients simultaneously at several regions at once. Image sequences were acquired for 2 seconds at frequency of 1 kHz with the acquisition system described in Chapter 2.

As shown in **Fig.3.1B**, when three APs were elicited in a T cell (displayed in **Fig 3.1A**), the optical signal $\Delta F/F$ was approximately 6 % both in the soma and in the two axons innervating the skin. Successive action potentials elicited by somatic injection of current pulses produced distinguishable episodes of calcium entry. $\Delta F/F$ increased in steps, each step associated with the occurrence of an individual AP. The rise of the optical signal followed the peak of the AP by about 1 or 2 msec (see **Fig.3.1B**). After reaching a peak, $\Delta F/F$ declined to zero with a time constant of about 1.6 sec in the soma and 1.4 and 1 sec in the axons. As in barnacle neurons the recovery time was shown to be faster in the neuropil than in the soma or axon (Ross et al. 1986). The time course of decay of the fluorescence signal from the soma of a typical cell was exponential, (Ross et al. 1986). The membrane time constant, τ, represents the time for the calcium concentration to fall to 63% of its final value but is not a true measure of the removal of calcium in the cell, since the dye acts as a buffer (Gorman and Thomas, 1980).

Fig.3.1C reproduces the spatial profile of ΔF/F in a colour-coded scale at four selected times (indicated by t_1 t_2 t_3 t_4 in panel **B**) after current injection: the optical signal increases almost uniformly and simultaneously in the distal processes.

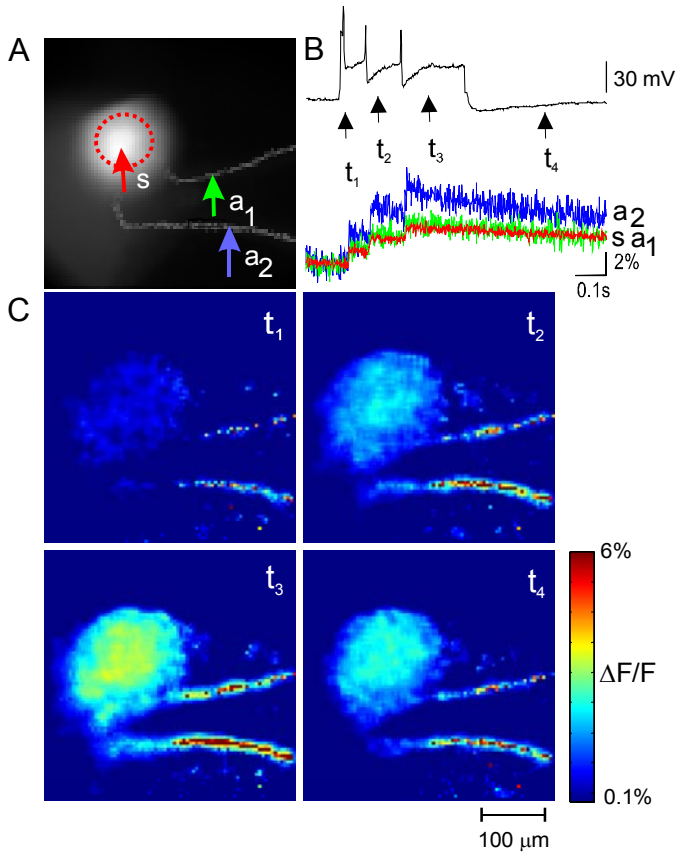

Figure 3.1 Calcium transients (ΔF/F) in a T cell. A: image of a T cell at 80x80 resolution. B: APs recorded from the soma with an intracellular microelectrode (black trace) and ΔF/F at three selected locations indicated in A with the same colour and lettering. The optical signal from the soma was averaged over the area encircled by the dotted red points in A. C: spatial profile of ΔF/F at four different times t_1, t_2, t_3 and t_4 (indicated in B) following electrical stimulation of the T cell with a depolarizing current pulse. The colour-coded scale is shown on the right. Th_1=1% Th_2 =3%. Data obtained from a single trial.

A more quantitative analysis of ΔF/F elicited by a single AP in mechanosensory neurons is shown in the P cell illustrated in **Fig.3.2A**, in which optical signals ΔF/F of about 3.5 % were observed at the locations indicated. ΔF/F followed the peak of the AP within 1 or 2 msec. The time constant τ of the decay of ΔF/F (see **Fig.3.2B**) varied between 1 and 2 seconds similarly to results previously obtained in Retzius cells (Beck et al. 2001). **Fig.3.2C** reproduces the spatial profile of ΔF/F in a colour-coded scale at four selected times (indicated by t_1 t_2 t_3 t_4 in panel **B**) after evoking a single AP in the P cell: the optical signal increased almost simultaneously in the soma and at some specific locations along the axon. A larger increase was observed in a sub-compartment of the soma (see red spots in images taken at t_1 and t_2 of panel **C**). When the optical signal in the soma was averaged over the circle indicated in panel **A**, ΔF/F had an amplitude and time course very similar (see panel **B**) to that observed at the two locations indicated in green, a_a, and blue, a_b, along the axon (see panel **A**). In control experiments the calcium indicator Calcium Green was used instead of Oregon Green and similar results were obtained, as shown in **Fig.3.2D**. In this experiment a P cell was loaded with Calcium Green and a single AP was evoked (see upper trace of panel **D**); Optical signals ΔF/F were measured on the cell body (red trace and s in panel **D**) and along the axon at about 40 μm (green trace and a_a in panel **D**) and at about 150 μm (blue trace and a_b in panel **D**) from the cell body. As Oregon Green emits fluorescence more efficiently than Calcium Green and the same light intensity was used in the two experiments, a similar emitted fluorescence can be explained by a larger loading of the dye Calcium Green. As shown in **Fig.3.2**, amplitude and time course of optical signals ΔF/F obtained with Oregon Green or Calcium Green were similar, suggesting that dye loading had a minor effect on calcium dynamics. Data from 4 P cells (red symbols), 1 T cell (black symbols) and 1 N cell (blue symbols) are shown in **Fig.3.2E**: the peak of the optical signal ΔF/F evoked by a single

AP had almost the same amplitude in the soma and along the axons at distances of 250 micrometers from the soma.

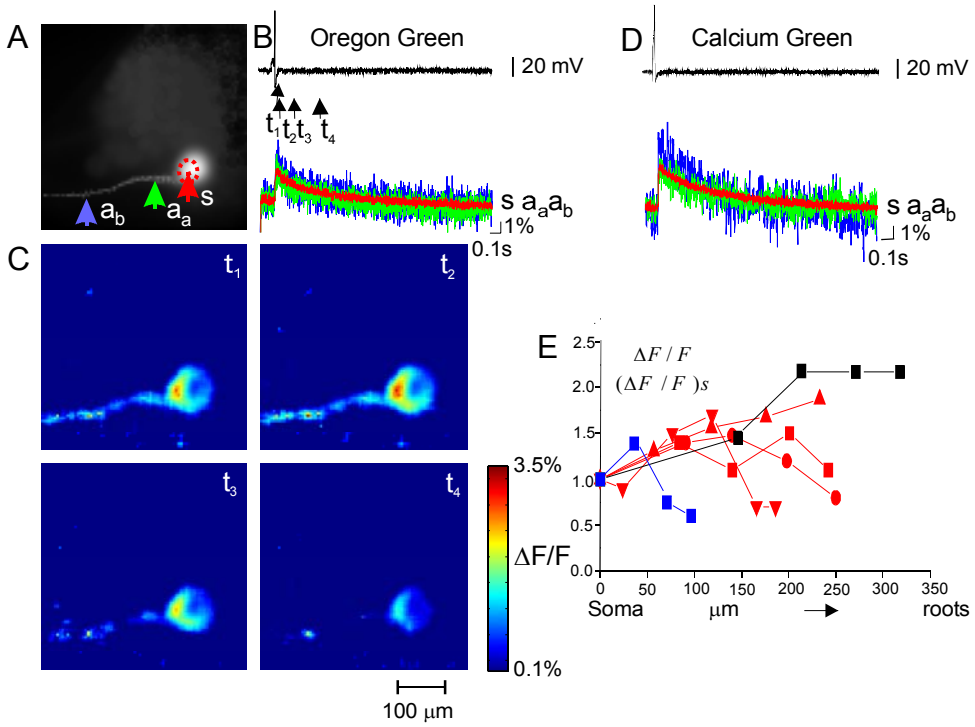

Figure 3.2 Calcium transients (ΔF/F) in mechanosensory neurons evoked by a single AP. A: image of a P cell at 80x80 resolution. B: a single AP recorded from the soma with an intracellular microelectrode (black trace) and time course of florescence changes (ΔF/F) at three selected locations indicated in A with the same colour and lettering. The optical signal from the soma was averaged over the area encircled by the dotted red points in A. C: spatial profile of ΔF/F at four times t_1, t_2, t_3 and t_4 (indicated in B) following electrical stimulation. The colour-coded scale is shown on the right. Th_1=1% Th_2 =2%. D: as in B but for P cell stained with Calcium Green and not Oregon Green. The location of the three selected locations where fluorescence changes (ΔF/F) were monitored are very similar to those indicated in panel A with the same colour. E: amplitude of the peak of ΔF/F recorded at different distances from the soma for 4 P (red symbols), 1 T (black symbols), and 1 N (blue symbols) mechanosensory neurons. Same symbols correspond to data obtained from the same mechanosensory neuron. Data obtained from single trials.

3.2 Skin stimulation

APs in mechanosensory neurons can be initiated either by direct mechanical stimulation of the skin (Nicholls and Baylor 1968), by extracellular stimulation of the roots (Nicholls and Baylor 1968; Wittenberg et al. 1990) or by intracellular stimulation of the cell body. In order to compare previous results obtained by the intracellular stimulation with the optical responses to a natural stimulus, we performed a following experiment. Skin preparation was made, consisting of a segment of the skin and a single ganglion innervating it. After the loading of the single mechanosensory neuron with the dye and a period of incubation, the skin was stimulated electrically, applying the current through the suction electrode and sequence of images was acquired. In **Fig 3.3A**, image of the P neuron is shown indicating the areas in which the time courses of relative fluorescence changes were evaluated. These time courses are displayed in the **Fig 3.3B** in the corresponding colours. **Fig.3.3C** reproduces the spatial profile of $\Delta F/F$ in a colour-coded scale at four selected times (indicated by t_1 t_2 t_3 t_4 in panel **B**) after the skin stimulation: the optical signal increases almost uniformly and simultaneously in the visible portion of the processes and in the cell body and reveals increases in the intracellular calcium concentration in response to skin stimulation that caused a depolarisation.

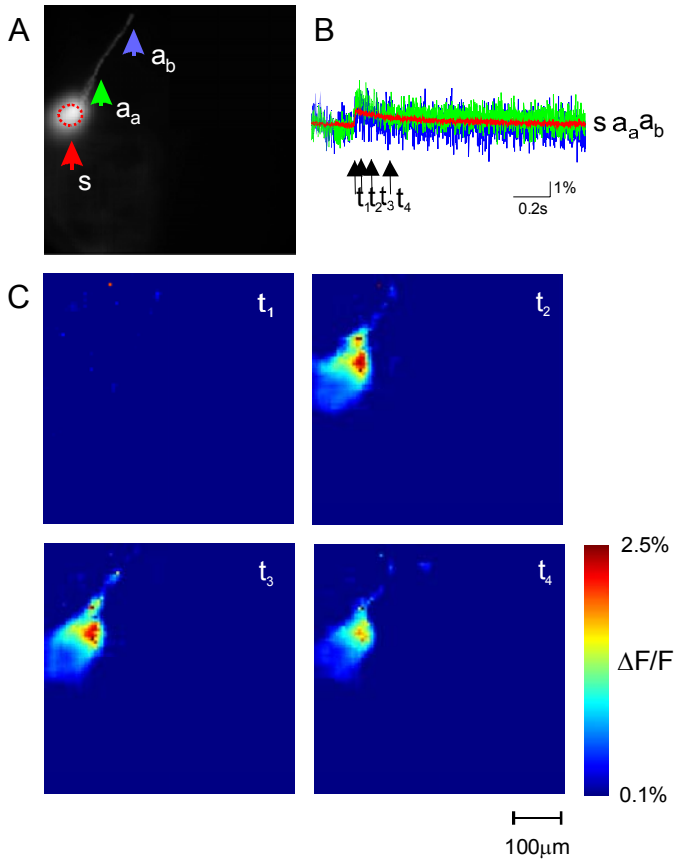

Figure 3.3 Calcium transients (ΔF/F) in P neuron evoked by a single AP induced by a skin stimulation. A: image of a P cell at 80x80 resolution. B: time course of florescence changes (ΔF/F) at three selected locations indicated in A with the same colour and lettering. The optical signal from the soma was averaged over the area encircled by the dotted red points in A. C: spatial profile of ΔF/F at four times t_1, t_2, t_3 and t_4 (indicated in B) following electrical stimulation. The colour-coded scale is shown on the right.

The time course of ΔF/F and the increases in the intracellular calcium concentration in the cell bodies and in the processes of the mechanosensory neurons, when the AP was initiated either in the soma or in the distal processes after the skin stimulation, were similar and almost indistinguishable.

3.3 Comparison of averaged and single trial responses

The data shown in **Figs 3.1** and **3.2** were obtained from single trials and were not averaged. In order to analyse reproducibility of calcium transients, mechanosensory neurons were loaded with Oregon Green and a single AP was evoked in successive trials, repeated every 2 minutes.

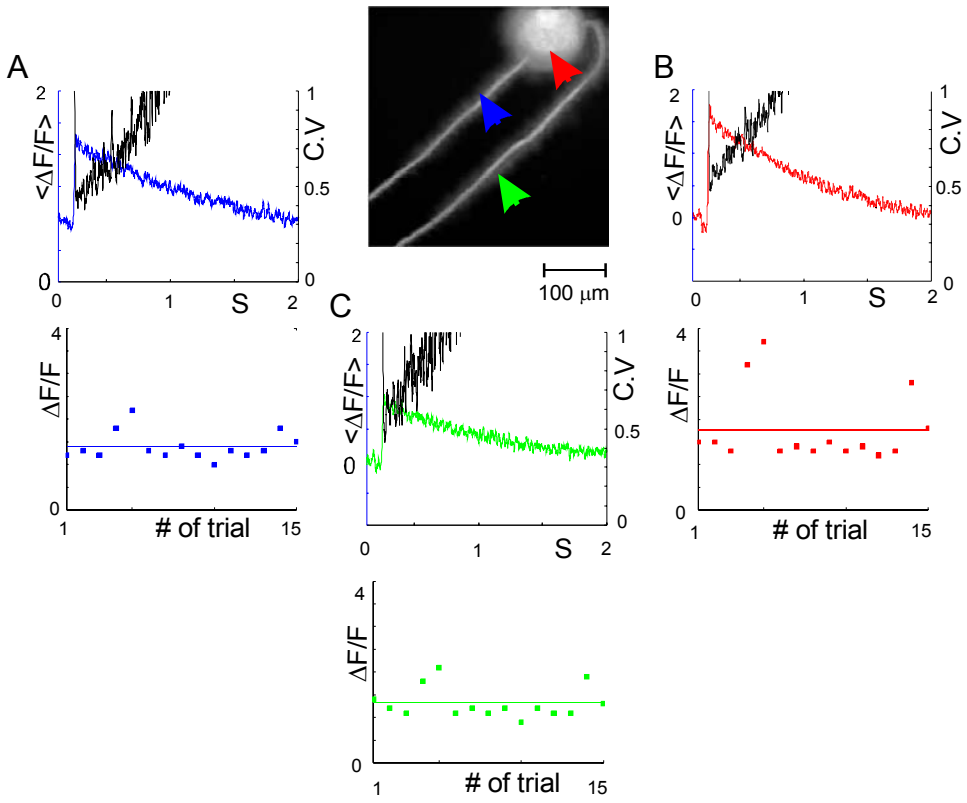

Figure 3.4 Reproducibility of calcium transients (ΔF/F) in mechanosensory neurons. At the centre of the figure there is an image at 80x80 resolution of a T cell. In A, B and C are shown the amplitude of the peak of ΔF/F in successive 15 trials and the average optical signal <ΔF/F> and its coefficient of variation $CV_{\Delta F/F}$ obtained from the three coloured regions of the neuron shown at the centre of the figure. The red colour and the letter s correspond to the soma and the blue and green colours and the lettering a_1 and a_2 corespond to the anterior and posterior axons, respectively. The $CV_{\Delta F/F}$ was computed as the ratio between the standard deviation of the optical signal $\sigma_{\Delta F/F}$ and <ΔF/F>. A single AP was evoked in each trial by injecting a brief depolarizing current pulse in the soma.

Figure 3.4 illustrates a stained T cell in which a single AP was evoked in 15 successive trials. Optical signals from the cell body (shown in red and with the letter s) and the two axons emerging from it (shown in blue, a_1, and green, a_2) were recorded. The amplitude of the peak of ΔF/F was stable over most trials, as shown in the lower portion of panels **A**, **B** and **C**. In two trials (# 4 and 5) large optical signals were observed, but in the remaining 13 trials the amplitude of ΔF/F was reproducible. The standard deviation of the peak of ΔF/F was 0.95, 0.48 and 0.53 in the soma and in the anterior and posterior axon. The average optical signal <ΔF/F> and its coefficient of variation $CV_{\Delta F/F}$ obtained from the three coloured regions of the neuron were computed. As shown in the upper portion of panels **A**, **B** and **C** the amplitude and time course of the averaged ΔF/F in the three regions were quite similar. The $CV_{\Delta F/F}$ in the axons decreased to about 0.4 at the peak of the optical signal and was 0.55 in the cell body. Very similar results were obtained in two other T cells, in three P cells and in two N cells. A coefficient of variation between 0.3 and 0.5 is often observed for electrical signals in many neuronal networks (Shadlen and Newsome 1994 and 1998) and is usually taken as an indication of good reproducibility.

3.4 Retzius cells

Calcium transients in subcompartments of the Retzius neurons as induced by single action potentials were studied by Beck et al. 2001. After intracellular stimulation of one Retzius cell, optical response from the other Retzius cell may be different. **Fig 3.5B**, black trace, shows APs from the soma of Retzius neuron labelled with green in A, recorded with an intracellular microelectrode. Lower traces show time course of florescence changes ($\Delta F/F$) of two Retzius cell bodies indicated in A with the same colour and lettering. These traces show that three APs of one Retzius cell induced only two APs in the other electrically coupled Retzius cell. **Fig 3.5D** and **F** show that APs induced a calcium transients of the same size in submembrane regions as in more central regions of the both Retzius cell bodies. Colours in **D** and **F** correspond to those in **C** and **E**.

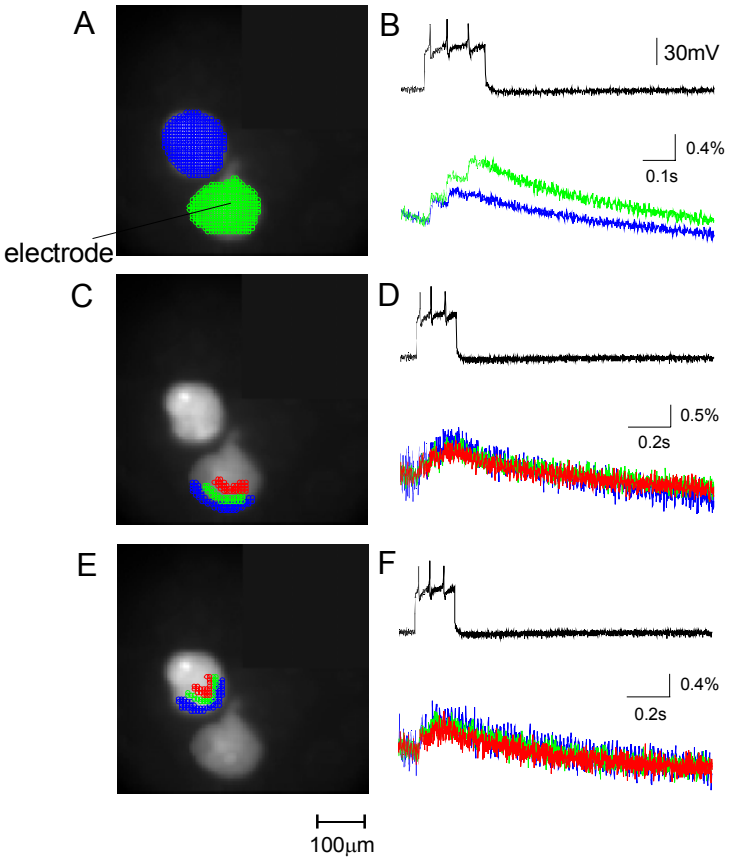

Figure 3.5 Calcium transients (ΔF/F) in Retzius cell bodies, where both cells were injected with dye. A, C and E: image of a Retzius cell bodies at 80x80 resolution. B: APs recorded from the soma with an intracellular microelectrode (black trace) and ΔF/F at two Retzius cell bodies indicated in A with the same colour and lettering. The optical signals from the soma were averaged over the area encircled by the dotted points in A. D and F: APs recorded from the soma with an intracellular microelectrode (black trace) and ΔF/F at three different regions of interest indicated in C and E with the same colours.

4 Calcium dynamics in motoneurons

4.1 Annulus Erector (AE)

4.1.1 Introduction

The Annulus Erector (AE) motoneuron innervates muscles immediately under the skin and its electrophysiological properties have been extensively investigated in previous studies (Gu et al. 1991). The AE motoneuron has a structure typical of several other known leech motoneurons. It has unipolar process emerging from the soma between 100 and 200 micrometers long (see Fig.5A). From the trunk, many fine branches emerge rich in postsynaptic contacts (Gu et al. 1991). The trunk divides at the first major bifurcation into two branches. The two branches project into the left and right contralateral roots and innervate specific muscles that cause annuli surrounding the animal to form ridges. Laser axotomy has shown that AE is not excitable along its axon proximally to the initiation zone that is in the region of the first major bifurcation, situated in the neuropil (Gu et al., 1991). Action potentials generated there spread only electrotonically into the soma, so the impulses generated in soma are small (Kuffler and Potter, 1964; Lytton and Kristan, 1989; Gu et al., 1991).

4.1.2 Results

To study motoneurons, I used the same experimental set-up as for mechanosensory neurons. This experimental set-up allowed recording of calcium transients simultaneously at several regions of interest. Image sequences were acquired for 2 seconds at frequency of 1 kHz with the acquisition system described in Chapter 2 and analyzed as explained in Section 2.4.

Fig.4.1B illustrates APs recorded in the soma after a pulse of depolarizing current was injected. These APs had an amplitude of about 5 mV. The red and blue traces reproduce the changes of ΔF/F recorded at the two different coloured locations shown by corresponding lettering in **Fig.4.1A**. In contrast with mechanosensory neurons, ΔF/F was significantly larger in the dendritic tree than in the soma where ΔF/F was negligible. At the first major bifurcation (indicated in blue and with the letter b) ΔF/F increased in discrete steps, each evoked by an individual AP. The size of each step was about 1.5%. The increase of ΔF/F in the first major bifurcation occurred with a delay of some msec from the peak of the AP recorded in the soma.

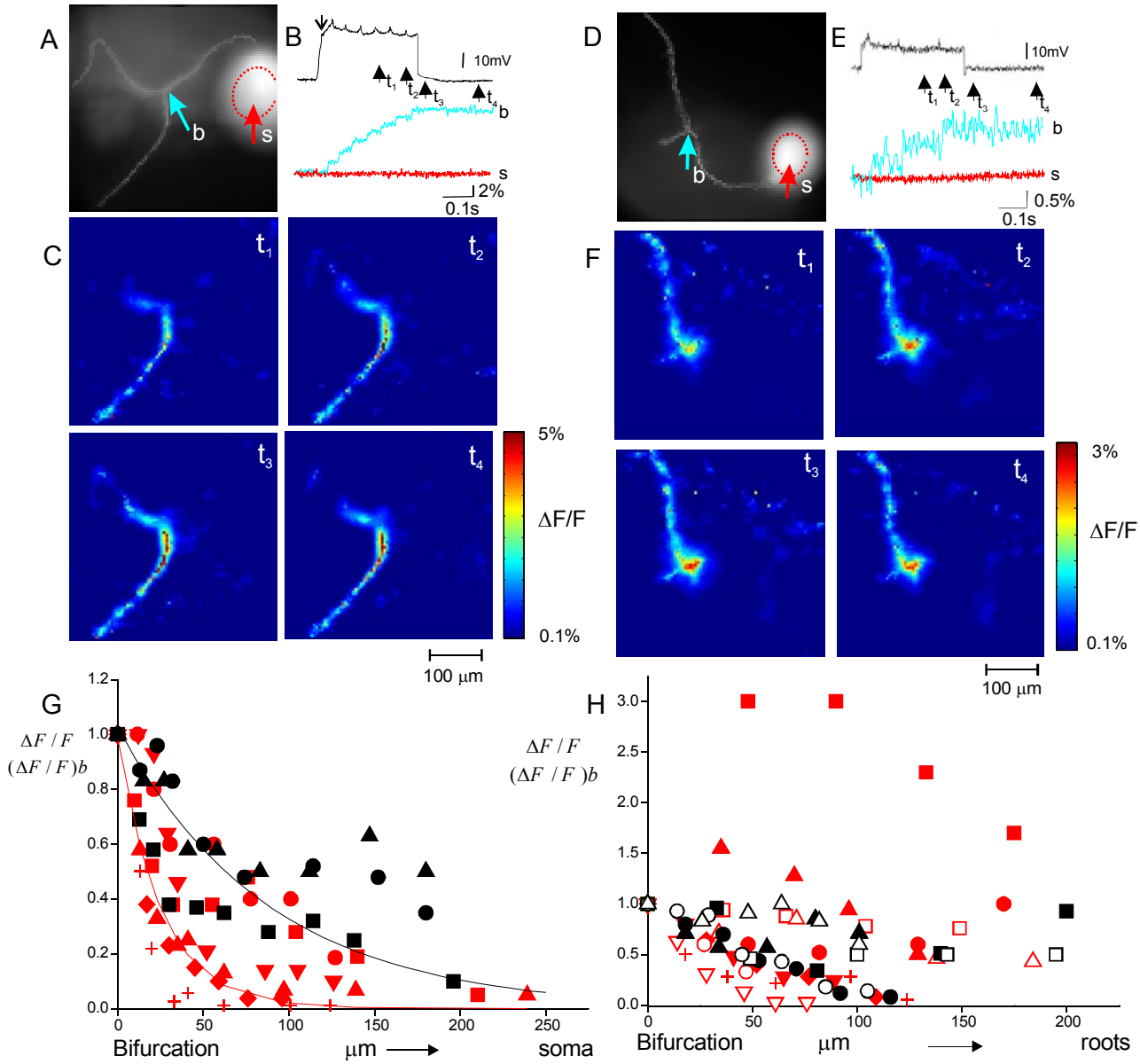

Figure 4.1 Calcium transients (ΔF/F) in an Annulus Erector motoneuron and in an Anterior Pagoda neuron: A: 80x80 image of the stained AE motoneuron. B: ΔF/F from the locations indicated with the same colour and lettering in A, and in black the voltage measured in the soma while passing a depolarizing current pulse. C: spatial profile of ΔF/F at different times following electrical stimulation. The colour-coded scale is shown on the right. Th_1=1% Th_2 =2%. D: 80x80 image of the stained Anterior Pagoda neuron. E: ΔF/F from the locations indicated with the same

colour and lettering in D, and superimposed in black the voltage recordings measured in the soma while passing a depolarizing current pulse. F: spatial profile of ΔF/F at different times following electrical stimulation. The colour-coded scale is shown on the right. Th_1=0.5% Th_2 =2%. G: amplitude of the peak of ΔF/F recorded at different distances from the bifurcation towards the soma. 6 Annulus Erector motoneurons (red symbols); 3 Anterior Pagoda neurons (black symbols) H: amplitude of the peak of ΔF/F recorded at different distances from the bifurcation towards the roots. Open and filled symbols refer to the ventral and anterior root respectively. The cross refers to one experiment in which only the branch projecting to the ventral root was stained. Data obtained from single trials.

Fig.4.1C illustrates images of changes of ΔF/F in a colour-coded scale at selected times after the current injection. ΔF/F is very small in the soma and in the initial portion of the trunk originating from it. On the contrary ΔF/F is visible and significant at the first major bifurcation and at all more distal locations. The amplitude of ΔF/F had a hot spot at the first major bifurcation and was uniform in the more distal regions.

4.2 Anterior Pagoda

4.2.1 Introduction

The Anterior Pagoda is a neuron extensively analysed in previous investigations (Melinek and Muller 1996). Its function is not known. It has a unipolar process with a major bifurcation 150/200 micrometers distally from the soma. The two major branches project into the anterior and posterior contralateral roots (see **Fig 4.1D**). APs recorded in the soma have an amplitude varying between 5 and 10 mV with a characteristic shape (reminiscent of the roof of a

pagoda). As with the AE motoneuron, the site of initiation of APs has been identified at the first major bifurcation (Melinek and Muller 1996).

4.2.2 Main results

When a pulse of depolarizing current was injected through the microelectrode into the soma, a train of small APs was evoked, as shown in **Fig.4.1E**. The coloured traces in **Fig. 4.1E** indicate that ΔF/F in the soma was almost undetectable, while it became visible at the first major bifurcation 150 microns distal from it. At the first major bifurcation (indicated in blue and with the letter b) ΔF/F increased in discrete steps, each evoked by an individual AP. The size of each step was about 0.5%. **Fig. 4.1F** illustrates images of changes of ΔF/F in a colour-coded scale at selected times after the current injection. ΔF/F is very small in the soma and in the initial portion of the major axo-dendritic tree originating from it. ΔF/F was significantly larger on locations more distal than the first major bifurcation. Similar results were obtained from a total of 5 Anterior Pagoda neurons.

The decline of ΔF/F along the initial trunk connecting the first bifurcation to the soma is analysed in **Fig.4.1G**, where red and black symbols refer to data collected from the Annulus Erector and the Anterior Pagoda neurons respectively. ΔF/F declined rather sharply with a space constant varying from 25 to 90 μm (see the solid lines in red and black in panel G). The decline of ΔF/F along the initial portion within the trunk is in sharp contrast with what was observed in mechosensory neurons (see **Fig. 3.2D**) where the amplitude of ΔF/F in the soma and in the axons

was almost uniform. The change of ΔF/F along the branches from the first major bifurcation towards the roots is reproduced in **Fig.4.1H** for the two branches (open and filled symbols) of Anterior Pagoda and AE neurons. In some cases ΔF/F clearly declined, but in other neurons, ΔF/F in distal branches was large and comparable with that observed at the bifurcation.

The small optical signal recorded in the soma compared to that observed at the first major bifurcation and in distal processes could be due to an inhomogeneous loading of the dye and/or to a dye sequestration into intracellular organelles of the soma of the Anterior Pagoda and AE neurons. As shown in **Figs 2.2** and **4.1** the soma of motoneurons is well stained and its resting fluorescence was comparable to that of mechanosensory neurons as those shown in **Figs 3.1** and **3.2**. In two experiments optical signals from the soma were measured while injecting the dye. In these two experiments ΔF/F in the soma was also small and almost undetectable. In these experiments optical signals were measured as soon as the soma appeared to be stained when the dye was presumably in the cytoplasm before it could have been absorbed by intracellular stores. These observations suggest that the compartmentalization of calcium transients in the Anterior Pagoda and AE neurons is physiological and is not due to inhomogenity of dye loading and/or to its sequestration into intracellular stores.

4.2.3 Differential invasion of APs in branches

The results described in the previous section were obtained from single trials and it is possible that the invasion of distal processes following stimulation of the cell body may vary

from trial to trial. Therefore, the reproducibility of calcium transients in the AE motoneuron was studied in successive trials.

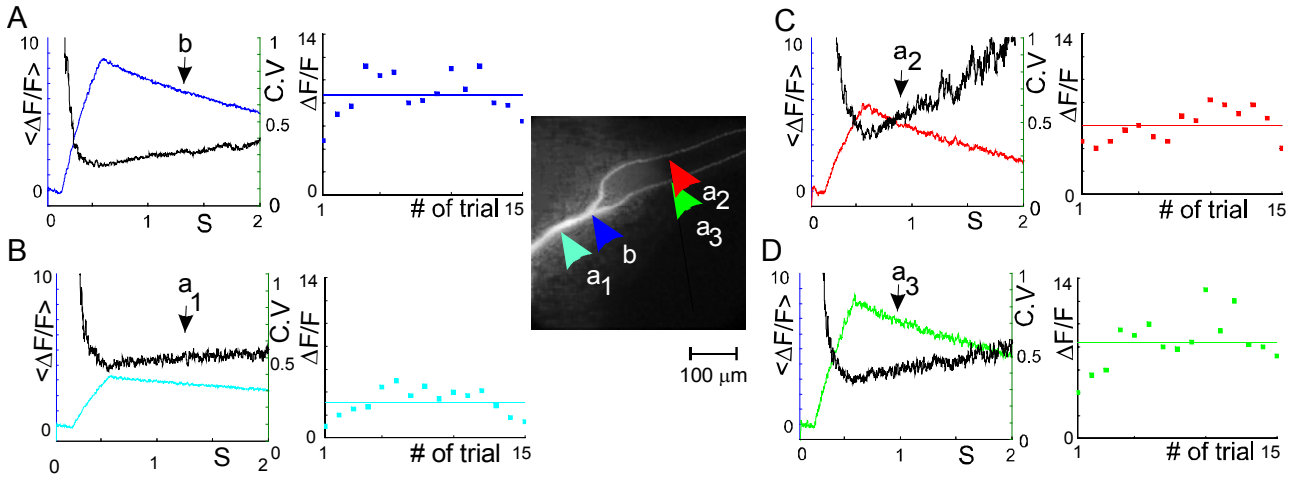

Figure 4.2 Reproducibility of calcium transients (ΔF/F) in the AE motoneuron. At the centre of the figure there is an image at 80x80 resolution of an AE motoneuron. In A, B, C and D are shown the amplitude of the peak of ΔF/F in successive 15 trials, the average optical signal <ΔF/F> and its coefficient of variation $CV_{\Delta F/F}$ obtained from the four coloured regions of the neuron shown at the centre of the figure. The cyan colour and a_1 correspond to the trunk, the blue colour and b to the first major bifurcation, red, a_2, and green, a_3, to the anterior and posterior processes, respectively. The $CV_{\Delta F/F}$ was computed as the ratio between the standard deviation of the optical signal $\sigma_{F/F}$ and <ΔF/F>. A train of 6 or 7 APs was evoked in each trial by injecting a depolarizing current pulse in the soma. Therefore, the time to reach the peak of ΔF/F is longer than in the experiments shown in Fig.4 where a single AP was evoked in each trial. Same motoneuron as in Fig.4.1

Fig.4.2 illustrates a stained AE motoneuron in which trains of 6 or 7 APs were evoked in successive trials. Optical signals from the first major bifurcation (shown in blue and with the

letter b), the trunk connecting the bifurcation to the cell body (shown in cyan and with a_1) and the two processes emerging from the first major bifurcation (shown in red, a_2, and green, a_3) were recorded and their variability analysed. In all trials calcium transients were larger at the first bifurcation and were detected in both processes: indeed, the amplitude of the peak of $\Delta F/F$ was very similar in all trials, as shown in the left portion of panels **A, B, C** and **D**. The average optical signal $<\Delta F/F>$ and its coefficient of variation $CV_{\Delta F/F}$ obtained from the four coloured regions of the motoneuron were computed. As shown in the right portion of panels **A** and **B**, in all trials $<\Delta F/F>$ in the trunk was approximately 3 times smaller than at the first major bifurcation. In all trials optical signals were observed, with an average amplitude of 5.9 % and of 8.4 % in the anterior and posterior branches, respectively. The $CV_{\Delta F/F}$ at the first major bifurcation decreased to about 0.3 at the peak of the optical signal and was less than 0.5 in the two branches. Similar results were obtained in two other AE motoneurons and in one AP motoneuron. These results indicate that calcium transients are detected equally well in the two branches emerging from the first major bifurcation and that calcium dynamics is rather reproducible in leech motoneurons.

4.2.4 The effect of steady currents

The initiation site of APs in the AE and in the Anterior Pagoda neurons, can be modulated by steady currents injected into the soma (Gu et al. 1991; Melinek and Muller 1996). Thus depolarising currents move the initiation site towards the soma and hyperpolarizing current moves it towards the roots.

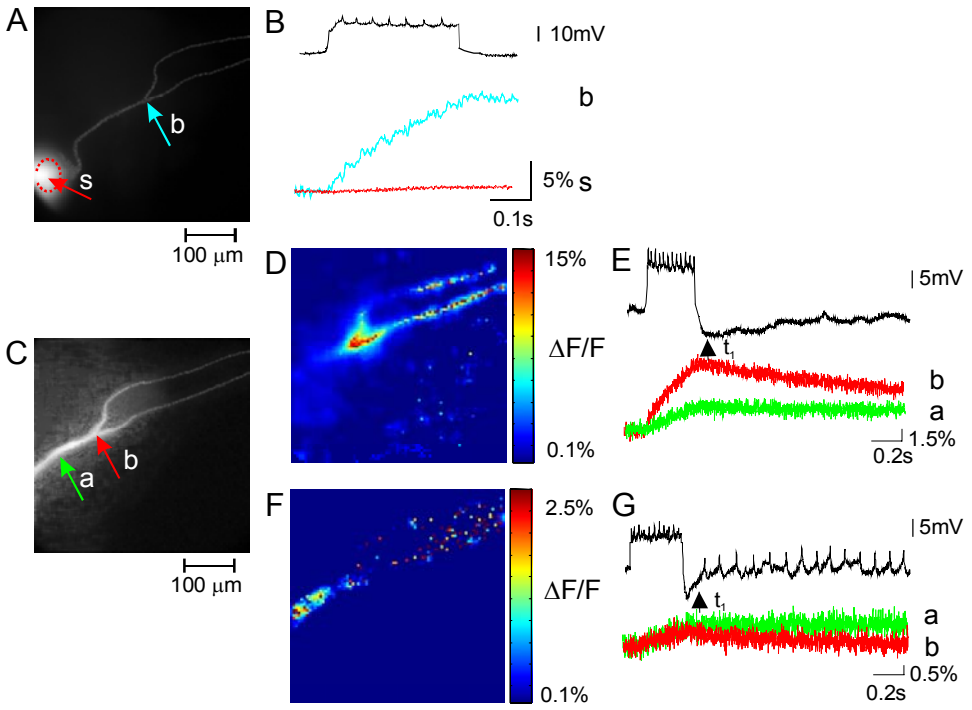

Figure 4.3 The effect of steady currents on the amplitude of calcium transients (ΔF/F) in the same AE motoneuron as in Fig.6. A: Image of the AE motoneuron with its cell body fully visible. B: time course of ΔF/F measured at the locations indicated with the same colour and the lettering in A. The black trace is the voltage recorded in the soma while passing a depolarising current pulse. C: Image of the same AE motoneuron when more distal branches were viewed. D: spatial profile of ΔF/F in the absence of the depolarising steady current. E: ΔF/F from the locations indicated with the same colour in C and superimposed, in black, the voltage recorded at the soma. F: spatial profile of ΔF/F in the presence of a steady depolarising current. G: as in E but in the presence of a steady depolarising current of the same amplitude as that used in panels D and E. In F and G the reference value for F was that achieved with the steady current. Data obtained from single trials.

A large optical signal was recorded at the first major bifurcation of the AE neuron shown in **Fig.4.3A**, but no detectable fluorescence changes were measured in its soma (see **Fig. 4.3B**).

This was also true when a train of 7 APs were elicited by passing a depolarizing current pulse through the microelectrode inserted in the soma. Having established that optical signals in the soma were negligible, the preparation was moved by about 100 micrometers and a large portion of the distal dendrites was visualized (see **Fig.4.3C**). When 12 APs were evoked in the neuron (see **Fig.4.3E**), a large optical signal ΔF/F with an amplitude of approximately 15 % was observed at the first major bifurcation (see red trace in **Fig. 4.3E**). As shown in panels **D** and **E,** a much smaller optical signal was detected along the trunk. When a steady depolarizing current was injected through the microelectrode, the AE neuron fired a train of APs with a frequency of 10 Hz and the firing rate increased to 30 Hz when the same depolarising current pulse was superimposed to the steady current (see **Fig.4.3G**). Under these conditions, as shown in **Fig. 4.3F** and **G**, the optical signal ΔF/F evoked by the same depolarising pulse was very similar in the bifurcation and in the trunk. When a steady hyperpolarizing current was injected, optical signals elicited by a depolarizing pulse evoking a brief train of APs, were primarily located at the first bifurcation, in accord with what was observed in the absence of a steady current. Similar results were obtained from a total of 6 AE motoneurons, showing that the region of calcium transients was moved towards the soma by a steady depolarization.

These results show that APs evoked in the Annulus Erector motoneuron cause intracellular Ca^{2+} to increase at locations more distal than the first major bifurcation, at a position identified as the initiation site of APs in previous studies (Gu et al. 1991). In the presence of a steady depolarising current, small but detectable Ca^{2+} transients were found in the trunk with an amplitude larger than those measured at more distal locations.

4.2.5 Comparison of calcium transients elicited by stimulation of the soma and distal processes

In order to establish the degree of compartmentalization of optical signals in the Anterior Pagoda neuron, calcium transients originated by direct intracellular stimulation of the soma and by extracellular stimulation of the roots (see **Fig.4.4A**) were compared.

The first major bifurcation and the distal dendrites were visualized (see **Fig.4.4A**). We compared ΔF/F when APs were initiated by passing a depolarizing current pulse in the soma (see **Fig. 4.4B** and **C**) and when APs were evoked by extracellular stimulation of the anterior (see **Fig.4.4 D** and **E**) or posterior root (see **Fig. 4.4 F** and **G**). As shown in the **Fig.4.4 C, E** and **G**, the stimuli evoked a train of a similar number of APs clearly detected by the intracellular microelectrode impaling the soma.

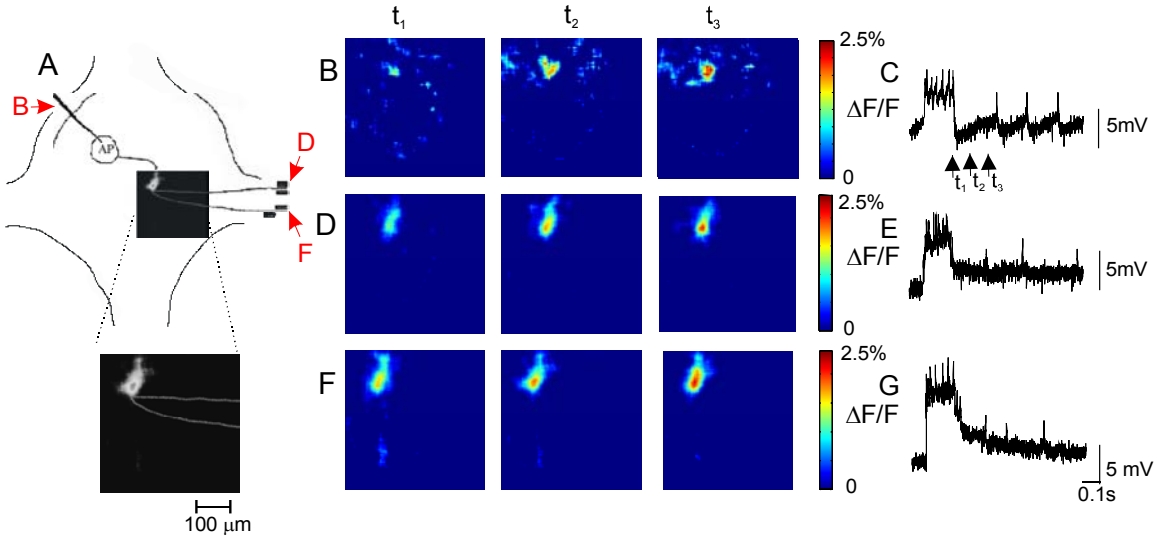

Figure 4.4 Comparison of calcium transients (ΔF/F) initiated by stimulation of distal roots and by injection of a depolarizing current in the soma. A: schematic drawing of a leech ganglion containing an image of the major bifurcation of the Anterior Pagoda neuron. The red letters (B, D and F) indicate the stimulation sites used in panels B and C, D and E and in F and G respectively. B: spatial profile of ΔF/F at different times following electrical stimulation of the soma. The colour-coded scale is shown at the right. C: intracellular recordings from the soma of the Anterior Pagoda neuron while passing a depolarizing current step in the soma. Evoked APs have an amplitude of about 5 mV. D: spatial profile of ΔF/F at different times following extracellular stimulation of the anterior root. E: intracellular recordings from the soma of an Anterior Pagoda neuron while stimulating extracellularly the anterior root. F: spatial profile of ΔF/F at different times following extracellular stimulation of the posterior root. G: intracellular recordings from the soma of an Anterior Pagoda neuron while stimulating extracellularly the posterior root. Data obtained from single trials.

For the three stimulations, the time course and spatial profile of ΔF/F was similar: in all three cases ΔF/F was significantly larger at the first major bifurcation (see panels **B, D** and **F**) and was small and almost undetectable in the soma. Calcium transients evoked by the stimulation of the anterior root propagated to the processes entering into the posterior root and vice versa, but were greatly attenuated at the soma.

4.2.6 L motoneuron and other motoneurons

The L motoneuron innervates longitudinal muscles in the leech skin and projects contralaterally into the anterior and posterior roots. Electrophysiological and functional properties of the L motoneuron have been well characterized. APs recorded in the soma have an

amplitude slightly larger than in the Annulus Erector and Anterior Pagoda neurons and vary between 5 and 10 mV (Stuart 1970).

In three L motoneurons we repeated the experiments described in **Fig.4.1** obtaining similar results: when APs were evoked in L motoneurons, ΔF/F was larger in distal processes than in the soma. This is shown in **Fig.4.5** where in **Fig. 4.5A** image of the stained L motoneuron is presented, in **Fig.4.5B** time course of florescence changes (ΔF/F) at four selected locations indicated in **A** with the same colour and lettering is presented, and **Fig.4.5C** illustrates images of changes of ΔF/F in a colour-coded scale at selected times after the current injection. Similar experiments were repeated in two motoneurons # 5 and in one motoneuron # 2, with very similar results. In all analysed motoneurons ΔF/F was significantly larger in distal processes than in the soma.

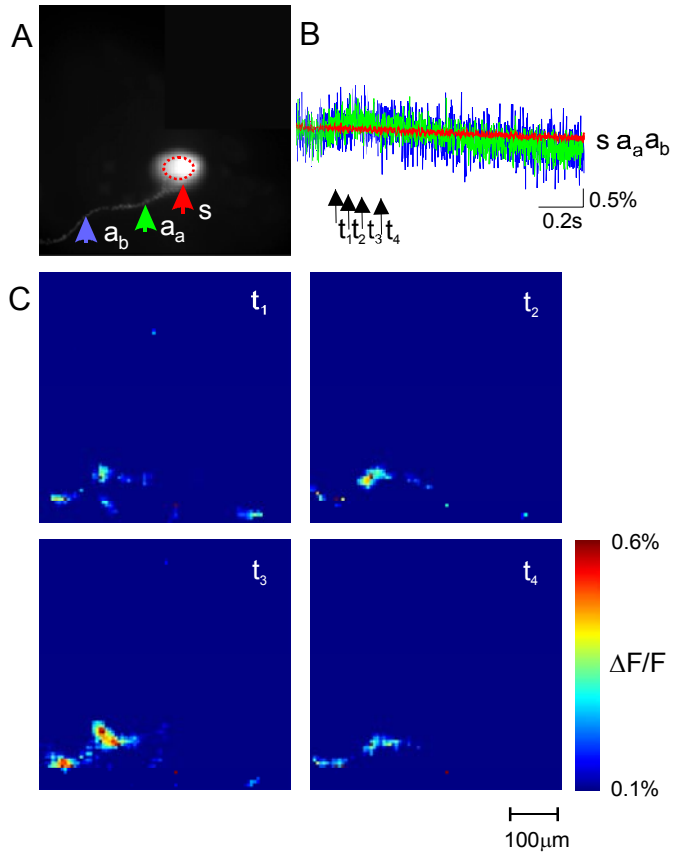

Figure 4.5 Calcium transients (ΔF/F) in an L motoneuron: A: 80x80 image of the stained L motoneuron. B: ΔF/F from the locations indicated with the same colour and lettering in A. C: spatial profile of ΔF/F at four different times t_1, t_2, t_3 and t_4 (indicated in B) following electrical stimulation. The colour-coded scale is shown on the right.

5 Discussion

5.1 Why the leech?

Information processing and functional compartmentalization of neurons are among the major questions of cellular and systems neuroscience investigations. In order to study these problems, we have used a preparation of leech ganglia. It satisfies the necessary requirement that experiments must be performed in at least partially intact neuronal structures, as leech ganglia are, in order to ensure that highly specific regional electrical properties of individual neurons and characteristic synaptic connections are preserved. Cells in different regions of the leech nervous system are diverse in their morphology and in their electrical and biochemical properties. Even a fundamental phenomenon such as the amplitude of action potentials, varies in shape and size in different neurons. In addition, the pattern of action potential firing exhibits great diversity in neurons. This diversity reflects differences in membrane ion channels, their kinetic properties, single channel conductance, density and voltage dependence. We have chosen the leech to study the role of single identified nerve cells in information processing and integration also because previous studies have provided a considerable quantity of detailed information about their morphological, physiological and functional properties (see Section 1.1).

5.2 Optical recording

It is difficult to understand the behaviour of many cells on the simple basis of simultaneous microelectrode measurements from the soma or from a few neural positions. To improve spatial resolution and achieve multi-site recording, it was necessary to turn to indirect measurements of voltage changes. Indeed, optical recording offers the possibility of recording from processes that are too small or fragile for electrode recording.

5.2.1 Voltage-sensitive dyes

To study signal integration, AP formation and propagation by using optical techniques that have a good spatial resolution, the best choice would be to use voltage-sensitive dyes (see Zochowski et al, 2000; Zecevic and Antic, 1998). In light of this, we did perform some preliminary experiments using these dyes. They indicated partial success in the effort to use intracellularly applied voltage-sensitive dyes to record responses from neurons in leech ganglion. The results suggest that, with further improvements, it may be possible to follow optically synaptic integration and spike conduction and consequently sodium and potassium ion channels distribution in leech neurons. However, these experiments show the advantages of selective staining of particular neurons by intracellular application of the dye. The two most serious problems were the slow diffusion of this dye and the low signal-to-noise ratio of the optical responses. Because the signal size was small, it was not possible to use multisite optical

recording to study the regional characteristics in leech single neurons. Limitations and prospects for a further refinement of the technique depend mostly on the signal-to-noise ratio; improvements in both the apparatus and the design of more sensitive dyes can increase the signal-to-noise ratio.

5.2.2 Calcium recording

Calcium indicators have been often used to image AP initiation in a variety of neurons and, although they have some disadvantages (Waters et al. 2005), they are a powerful tool to investigate compartmentalization at a cellular level and to monitor changes of intracellular Ca^{2+} concentration. The advantages and disadvantages of calcium indicators are recalled in the Section 2.3.2. As calcium influx is a secondary consequence of depolarisation, depends on the presence of voltage-sensitive calcium permeable channels and it is a twice remote indirect measurement of the membrane voltage, we monitored light and derived calcium concentration changes that are, in turn, related to changes in membrane potential. With this approach, we tried to give an answer to these questions: 1) If most leech neurons appear electrically compartmentalized, will it be the same for intracellular messengers such as calcium? 2) What are the functional implications of these biophysical properties?

But, there were several technical problems that we had to consider and they will be reported in this discussion. Calcium sensitive dyes are slow in comparison to voltage sensitive dyes so action potential shape and peak latency along the neuron cannot be followed. But the signal-to-noise ratio of calcium dyes is much more evident, enough to record optical signals from many locations in the neuron. These signals give information about the time course of the potential change but no direct information about its magnitude. In many measurements the

absolute calibration of optical signals in terms of voltage is not critical. Many conclusions depend on the comparison between relative amplitudes and time information that are obtained from nonratiometric optical recordings.

When calcium channels were expressed in the neural cell subcompartments, activation of these channels by depolarisation caused an increase in the intracellular calcium concentration. Since fluorescence change ($\Delta F/F$) is related to changes of intracellular Ca^{2+} (Jaffe et al. 1992; Stuart et al. 1997; Koester and Sakmann 2000; Waters et al. 2005), spatial and temporal properties of calcium dynamics were analysed at a fast temporal resolution (1 kHz) and at several simultaneous locations. Following impulses in each of the cells, clear, distinctive step increases of fluorescence were recorded. The changes in all cells were large enough to be detected in a single trial.

Measurements of rapid changes in intracellular calcium initiated by an electrical event, millisecond time scale, allowed us to study when, where and how much calcium has entered. Buffering prevents calcium from spreading by diffusion more than a few micrometers. The voltage signals spread and they cause calcium entry along the way. Since calcium diffuses slowly in cytoplasm compared to the time course of most electrically induced transients, different regions of a neuron respond independently to the changes in calcium and the site where calcium increases must be close to the channel location. Since the rising phase of a calcium transient was almost coincident in time with the electrical event that caused it, the detection of the transient can also be used as an indicator of an action potential. As calcium levels in neurons change in response to electrical events, knowledge of the time course, amplitude, and spatial distribution of calcium transients evoked by electrical activity can give information about the events that caused the changes (Ross, 1989). It is important to know how accurately the calcium

dye signals represent electrical events and this was done by comparing electrical signals with optically recorded signals. Electrophysiological recording of the membrane potential parallel to the optical recording showed that the optical response corresponded to the electrical change. A problem may arise if voltage-sensitive calcium channels are not present, whereupon an AP would not induce the entrance of the calcium in the cell. But in our experiments, this was not the case. The calcium response was absent only in the region where intracellular recording showed the size of APs was only 4-5 mV, which means that the region was not excitable and that the signal arrived there passively. So we have demonstrated that the calcium response follows the AP propagation and we have raised several questions: What is the role of calcium? Does it play a role in signal integration together with sodium and potassium, or does it play a second messenger role, connecting the electrical and chemical events? On the basis of the results, we can say that calcium transients in our experiments were fast, which probably means that they were mainly involved in information processing. Slower changes in calcium concentration would be probably involved in other functions.

Our experiments also provide several important methodological results. First, they show that it is possible to deposit the dyes into the cell without staining the surrounding tissue. The signal-to-noise ratio in fluorescence is degraded by the dye bound to extraneous material. It was possible to deposit the dye into the cell without staining the surrounding tissue, keeping low, in this way, the background fluorescence. In each ganglion, only one neuron was stained so fluorescence was coming only from cell of interest. In addition, we established that pharmacological effects of the dye were small and reversible. The absence of large pharmacological effects is evident from the fact that electrically recorded action potentials were essentially unchanged after staining and an incubation period of more than 2 hours. Furthermore,

photodynamic damage at the incident-light intensities used was not significant, since the time course of the electrically recorded action potentials from the cell body and optically recorded signals from the soma and the neuronal processes didn't change over several trials.

5.3 Calcium dynamics in leech neurons

A single AP in mechanosensory neurons evoked an optical signal ΔF/F with peak amplitude varying between 2 and 6 %. Optical signals ΔF/F of similar amplitude caused by a single AP backpropagating in the dendrites of CA1 pyramidal neurons (Callaway and Ross 1995; Spruston et al. 1995; Frick et al. 2003) and of neocortical pyramidal neurons (Markram et al. 1995) were observed. Larger optical signals evoked by a single AP were measured in the intact retina (Denk and Detwiler 1999). As shown in **Figs. 3.1 -3.4** the value of ΔF/F is similar in the soma, in the distal processes and in the branches innervating the skin. A similar behaviour is observed in many other mammalian neurons of the CNS, where calcium transients initiated by APs are observed with approximately the same size in the cell body and in dendrites like in CA1 pyramidal neurons (Frick et al. 2003). In L2/3 pyramidal neurons the peak value ΔF/F evoked by a single AP is about 10 % in the soma, increases by 2 or 3 times at a distance of about 100 μm along the apical dendrites, and it decreases at larger distances from the soma (Callaway and Ross 1995; Spruston et al. 1995; Waters et al. 2003, 2005).

The aim of this study was to elucidate how uniform these calcium transients are along the cellular processes and the soma, and how they modulate the shape of an AP. The results in **Figs 3.1** and **3.2** show that only minor differences in the amplitude of the calcium transients in different parts of the cell membrane have been found, indicating that the calcium influx is

distributed almost equally and that calcium transients, elicited by APs in mechanosensory neurons, have similar properties in the soma and in the axons. The time course marking the return of a calcium transient to baseline is indicative of the speed of buffering, sequestration, or pumping out of free calcium from cytoplasm. There is no a priori reason for assuming that all parts of the cell will respond in the same way. Our experiments have shown that recovery time was faster in the distal axon than in the soma that is in agreement with the results published on barnacle neurons (Ross et al. 1986). Our results indicate that AP induced intracellular calcium transients are mediated by the opening of voltage-gated channels in both dendrites and the soma. It is concluded that voltage gated Ca^{2+} channels are not differentially clustered along processes of mechanosensory neurons; and voltage signals and Ca^{2+} transients are observed throughout the entire neuron.

As shown in **Figs.4.1-4.5** in the Anterior Pagoda neuron, in the AE, L # 5 and # 2 motoneurons $\Delta F/F$ associated with APs occur at the first major bifurcation and sharply decline with a space constant varying between 25 and 80 μm along the part of the trunk connected to the soma. In these neurons, calcium transients can be observed only in distal processes and are strongly compartmentalized. It appears that under normal conditions, slow depolarizing voltage pulses applied to the soma are electrotonically spread into the processes with little attenuation. These depolarizing pulses initiate action potentials in the processes at remote sites that appear to be more excitable than the neighbouring segments.

Calcium transients were not observed in the soma of these neurons even when large depolarizing currents were injected into the soma itself (**Fig.4.1**) and therefore the absence of calcium transients in the presence of APs cannot be attributed only to the small electrical signals reaching the soma. These observations show that the density of voltage gated calcium channels

in the soma of these neurons is significantly lower than in distal processes. The sharp decline of Ca^{2+} transients along the initial part of the trunk is caused by the combination of several mechanisms: i - the restricted diffusion of Ca^{2+} ions along a narrow structure; ii – the absorption and buffering of diffusing Ca^{2+} ions by intracellular stores; iii - a differential distribution of Na^{+} and Ca^{2+} voltage gated channels along the trunk. A Ca^{2+} -activated K^{+} conductance that has been described in the processes of the Anterior Pagoda neuron (Wessel et al. 1999a) is likely to be a major determinant also for the attenuation of the amplitude of APs along the same structure, and therefore will reduce the Ca^{2+} inflow through voltage gated Ca^{2+} channels along the trunk. APs in motoneurons are expected to have the usual amplitude of approximately 70 mV and their initiation site has been located at the first major bifurcation (Melinek and Muller 1996). An AP, travelling from the first bifurcation to the soma is attenuated between 10 and 20 times over a distance of 100-200 micrometers, indicating an effective space constant of approximately 50 μm, similar to the decline of the optical signal $\Delta F/F$ (see **Fig. 4.1**). A space constant of 50 μm in an entirely passive cable can originate from a very high axial resistivity and from an unusually high membrane conductance (Rall and Agmon-Snir 1998). A space constant for the higher frequencies associated with the action potential depends also on the capacitance. For brief events, the current flow giving rise to the signal may end before the membrane capacitances become fully charged. This has the effect of reducing the spread of the potential along the fiber. In other words, for brief signals the effective space constant is less than for those of longer duration. It is also likely that active properties such as the Ca^{2+} -activated K^{+} conductance (Wessel et al. 1999a and b) contribute to the large attenuation of voltage and the associated calcium transients along the major trunk.

This compartmentalization is reminiscent of what is observed in several invertebrate preparations, such as in barnacle neurons (Ross and Krauthamer 1984; Krauthamer and Ross 1984) and in Aplysia neurons (Gorman and Thomas 1978), where the initiation site of APs is located at 100-200 μm from the soma. In vertebrates and in particular in mammalian neurons, the site of AP initiation is usually located in the axon at some distance from the soma (Stuart and Sakmann 1994; Stuart et al. 1997). In cerebellar Purkinje rat neurons the site of AP initiation has been localized at about 75 micrometers from the soma, at the first major axonal branch (Clark et al. 2005). In these neurons, however, the amplitude of the AP recorded in the soma is large, almost identical to that measured at the site of AP initiation, because it back propagates.

Our results show that in the leech nervous system calcium dynamics in mechanosensory neurons compared to the great majority of other neurons are different. Calcium dynamics in the Anterior Pagoda neuron, in the AE, L, #2 and #5 motoneurons and presumably in most other motoneurons and interneurons are highly compartmentalized and calcium transients are restricted to the distal processes and hardly reach the soma (see **Figs.4.1-4.5**). By contrast, calcium transients are observed over the entire arborisation of mechanosensory neurons (see **Figs.3.1-3.4**). This differential compartmentalization in leech neurons is observed consistently in different trials and is affected by a small variability (see **Figs 3.4** and **4.2**). Therefore, compartmentalization of calcium dynamics mirrors the compartmentalization of electrical events (Gu et al. 1991; Melinek and Muller 1996).

Our results show a clear compartmentalization of calcium dynamics in most leech neurons, in which the soma does not give propagating action potentials. In such cells, the soma, while not excitable, can affect information processing by modulating the sites of origin and conduction of AP propagation in distal excitable processes. The appearance and the different size

and kinetics of the AP induced calcium transients in the soma and dendrites of the leech neurons suggest an important role that calcium has in the local modulation of the propagation of APs. Local variation in voltage-dependent calcium entry during an AP may modulate electrical excitation, propagation of APs and different modes of synaptic and non-synaptic communication between that cell and the other cells in the nervous system.

Calcium sensitive dye recording, with the present sensitivity and temporal and spatial resolution, is a powerful tool for investigating the principles of signal integration in single neurons. One step toward understanding how sensory inputs lead to appropriate motor behaviour is to learn how individual neurons process sensory information. Studies in the leech suggest that changes in its behaviour can be explained, at least in part, by the alteration of firing patterns of selected neurons and muscles resulting from modulation of multiple ion conductances. Information gathered from this animal will therefore increase our understanding regarding general principles underlying the cellular basis of behaviour. Thus, after observing the functional significance of the calcium sensitive voltage channels for dendritic integration of multiple synaptic inputs in the leech, we can expect these dynamics to be important in other invertebrate and vertebrate nervous systems.

5.4 Functional implications

Mechanosensory neurons (see **Fig.5.1A**) differ from other leech neurons in many aspects: in fact, they integrate sensory input in the skin and send signals to other neurons in the same ganglion and in neighboring ganglia. Nervous signals generated in the skin are transmitted to the soma, at a distance of some millimeters apart, by the usual action potentials. These APs have to reach presynaptic endings in the ganglion and in neighboring ganglia and travel at short distance

from the soma. Therefore, the soma of leech mechanosensory neurons is close to the pathway where action potentials must travel.

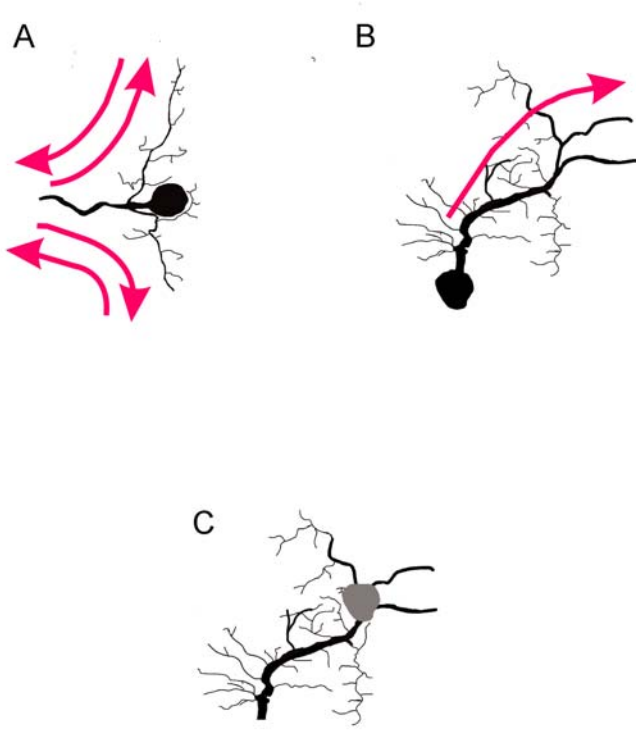

Figure 5.1 Electrical compartmentalization in leech neurons. A: in mechanosensory neurons, APs and the associated flow of information (indicated by red arrows) travel from the skin to the ganglion and vice versa. In mechanosensory neurons APs travel through the soma. B: in a unipolar motoneuron or interneuron, postsynaptic potentials are initiated in the fine branches emerging from the trunk. The flow of information (indicated by the red arrow) is conveyed by APs initiated at the first major bifurcation to the distal dendrites, where presynaptic terminals innervate muscles or second order neurons. In these neurons, the soma is distant from the main route of the information flow. C: in vertebrate neurons the soma (in grey) of unipolar leech neurons has been moved near the first major bifurcation.

Leech interneurons and motoneurons (see the scheme of **Fig. 5.1B**) need to integrate synaptic inputs within the ganglion itself. Leech interneurons and motoneurons obtain a

functional segregation of their processes by having many of their synaptic inputs concentrated between the soma and the first major bifurcation of their arborisation. Their presynaptic contacts to other neurons and/or muscles are primarily located more distally in relation to the first major bifurcation. In order to process properly some of the synaptic inputs, it is useful and possibly necessary to have a poorly excitable membrane with a low density of voltage gated Na^+ and Ca^{2+} channels, avoiding the initiation of action potentials which would temporarily wipe out all synaptic signals being passively propagated. Therefore, leech neurons have a low density of voltage-gated channels in those regions primarily destined for synaptic integration, i.e. between the soma and the first major bifurcation.

Leech motoneurons and possibly also interneurons achieve a functional segregation by controlling the density of voltage gated Na^+ and Ca^{2+} channels: their density is low in the soma, up to its first major bifurcation. The density of voltage-gated channels becomes high at the first major bifurcation, where APs are initiated. In leech interneurons and motoneurons, the flow of information goes from the trunk to the first bifurcation, where action potentials are initiated, and finally to the presynaptic endings in the ganglion or onto the muscles. The soma of the great majority of leech neurons has a low density of Na^+ and Ca^{2+} gated channels and, therefore, it is poorly excitable and does act as a threshold for incoming synaptic signals, as the soma of more conventional neurons does. Nonetheless, passive properties of the soma can influence the way in which APs travel on excitable distal processes, for instance by modulating their reflection at bifurcations (Baccus et al. 2000 and 2001) and by modifying the pattern of APs trains (Amir and Devor 2003; Amir et al 2005) with the occasional insertion of " extra APs ".

We believe that functional and anatomical properties of leech neurons and of vertebrate neurons, apparently so different, can be reconciled. The first major bifurcation has the same role

of the axon hillock of conventional vertebrate neurons. Vertebrate neurons, however, have developed a morphology which appears to be better suited to their functions and have the genetic and biochemical machinery (Craig and Banker 1994; Wodarz 2002) able to produce a polarized structure with distinct functional properties. In vertebrate neurons the soma of unipolar leech neurons has been moved to the major bifurcation, obtaining a better functional segregation with an excitable axon on one side and the dendritic tree on the other side (see **Fig. 5.1C**). However, we don't exclude that, by moving the soma to a location distant from the dendrites and axon hillock, the invertebrate neuron allows the site of integration to be closer to the region of synaptic input.

6. Conclusions

In my PhD thesis I addressed an important topic in cellular neuroscience: the functional compartmentalization of neurons. I studied the biophysical properties of single leech mechanosensory neurons and motoneurons and how they process information.

The experiments I performed aimed at investigating how and where action potentials arise and propagate into the arborizations of identified neurons in the leech nervous system. In particular, I investigated whether the entry of calcium is localized to distinct regions of the cells and whether there are significant differences in calcium channel distribution between different types of neurons.

The results presented in Chapter 3 show that in mechanosensory neurons the optical signal $\Delta F/F$ increased almost simultaneously in the soma and in locations along the axon, indicating that the voltage-gated calcium channels are not differentially clustered along processes; and voltage signals and calcium transients were observed throughout the entire neuron. The results in Chapter 4 show that in motoneurons, in contrast with mechanosensory neurons, $\Delta F/F$ was significantly larger in the dendritic tree than in the soma, where $\Delta F/F$ was negligible, indicating the strong compartmentalization; the density of calcium channels appeared to be much higher in the region of the first major bifurcation and distally from it, than in the region of the cell body.

The major achievement of my PhD project consists in the demonstration of compartmentalisation of calcium dynamics in leech neurons and that there are significant differences between different types of neurons. My experiments confirm and extend previous electrophysiological data, which demonstrate that the soma of motoneurons in the leech, as in

many other invertebrates, does not generate action potentials (Stuart, 1970; Muller and Nicholls, 1974). Thus at sites where APs are found to be large, the calcium signals are large, as in peripheral axons, whereas at sites where spikes are small, as in cell bodies of motoneurons, signals were small or non existent. These results indicate also a non uniform distribution of the voltage-sensitive calcium channels: calcium channels are distributed in a non-uniform manner over the surfaces of the motoneurons. Therefore, my results show a clear compartmentalization of calcium dynamics and of voltage-sensitive calcium channels in leech motoneurons. This pattern is consistent with measurements on many other preparations. In dendritic processes of these neurons, calcium channels contribute electrically to summing and spreading synaptic inputs.

The findings described above show the utility of an experimental approach combining optical recording with electrophysiological recording and image analysis, for studying the functional compartmentalization of neurons in a simple invertebrate system such as the medicinal leech.

Since biophysical properties of neurons in mammals and invertebrates are rather similar, understanding information processing in simple nervous systems provides a basis for unravelling mechanisms used by the brains of higher animals.

References

Amir R, and Devor M. Extra spike formation in sensory neurons and disruption of afferent spike patterning. *Biophysical J Neurosci* 84: 2700-2708, 2003.

Amir R, Kocsis JD and Devor M. Multiple interacting sites of ectopic spike electrogenesis in primary sensory neurons. *J Neurosci* 25(10): 2576-2585, 2005.

Andreasen M, Lambret DC. Regenerative properties of pyramidal cell dendrites in area CA1 of the rat hippocampus. *J Phisiol (Lond)* 483: 421-441, 1995.

Arisi I, Zoccolan D, Torre V. Distributed motor pattern underlying whole-body shortening in the medicinal leech. *J Neurophysiol* 86: 2475-2488, 2001.

Augustine GJ, Buchanan JA, Charlton MP, Osses LR, Smith SJ. Fingering the trigger for neurotransmitter secretion: studies on the calcium channels of squid giant presynaptic terminals. *Soc Gen Physiol Ser* 44: 203-23, 1989.

Baccus SA, Burrell BD, Sahley CL and Muller KJ. Action potential reflection and failure at axon branch points cause stepwise changes in EPDSPs in a neuron essenrtial for learning. *J Neurophysiol* 83: 1693-1700, 2000.

Baccus SA, Sahley CL and Muller KJ. Multiple sites of action potential initiation increase neuronal firirng rate. *J Neurophysiol* 86: 1226-1236, 2001.

Baader AP. Interneuronal and motor patterns during crawling behaviour of semi-intact leeches. *J Exp Biol* 200: 1369-1381, 1997.

Baylor DA, Nicholls JG. After effects of nerve impulses on signalling in the central nervous system of the leech. *J Physiol* 203:571-589, 1969.

Beck A, Lohr C, Deitmer JW. Calcium transients in subcompartments of the leech Retzius neuron as induced by single action potentials. *J Neurobiol* 48 (1): 1-18, 2001.

Beier SM, Barish ME. Cholinergic stimulation enhances cytosolic calcium ion accumulation in mouse hippocampal CA1 pyramidal neurones during short action potential trains. *J Physiol* 526: 129-42, 2000.

Blacckshaw SE. Morphology and distribution of touch cell terminals in the skin of the leech. J *Phisiol* 320:219-228, 1981.

Blacckshaw SE, Nicholls JG, Parnas I. Physiological responses, receptive fields and terminal arborization of nociceptive cells in the leech. *J Physiol* 326: 251-260, 1982.

Blacckshaw SE. Stretch receptors and body wall muscle in leeches. *Comp Biochem Physiol Comp Physiol* 105: 643-652, 1993

Blacckshaw SE, Nicholls JG. Neurobiology and development of the leech. *J Neurobiol* 27:267-276, 1995.

Callewaert G, Eilers J, Konneth A. Axonal calcium entry during fast 'sodium' action potentials in rat cerebellar Purkinje neurones. *J Physiol* 495 (Pt 3): 641-7, 1996.

Callaway JC and Ross WN. Frequency-dependent propagation of sodium action potentials in dendrites of hippocampal CA1 pyramidal neurones. *J Neurophysiol* 74(4): 1395-1403, 1995.

Clark BA, Monsivais P, Ranco T, London M and Hausser M. The site of action potential initiation in cerebellar Purkinje neurons. *Nature Neurosci* 8: 137-139, 2005.

Cline, Hollis T. 3H-GABA uptake selectively labels identifiable neurons in the leech central nervous system. *J Comp Neurol* 215 (3): 351-358, 1983.

Cohen MW, Jones OT, Angelides KJ. Distribution of Ca2+ channels on motor nerve terminals revealed by fluorescent omega-conotoxin. *J Neurosci* 11 (4):1032-9, 1991.

Combes D, Meyrand P. and Simmer, J. Motor pattern specification by dual descending pathways to a lobster-generating network. *J Neurosci* 19(9): 3610-3619, 1999a.

Combes D, Meyrand P and Simmer J. Dynamic Restructuring of a Rhythimc Motor Program by a Single Mechanoreceptor Neuron in Lobster. *J Neurosci* 19(9): 3620-3628, 1999b.

Craig AM. and Banker G. Neuronal Polarity. *Annu. Rev. Neurosci* 17: 267-310, 1994.

Denk W and Detwiler PB. Optical recording of light-evoked calcium signals in the functionally intact retina. *Proc Acad Sci USA* 96 (12): 7035-40, 1999.

Dolphin AC. Facilitation of Ca^{2+} current in excitable cells. *Trends Neurosci* 19: 35-43, 1996.

Dowling JE. Organisation of vertebrate retinas. *Invest Ophtamol* 9 (9): 655-80, 1970.

Dowling JE, Chapell RL. Neural organization of the medial ocellus of the dragonfly. II. Synaptic structure. *J Gen Physiol* 60: 148-65, 1972.

Duch Cand Levine RB. Remodeling of membrane properties and dendritic architecture accompanies the postembryonic conversion of a slow into a fast motoneuron. *J Neurosci* 20 (18): 6950-61, 2000.

Eilers J, Callewaert G, Armstrong C, Konnerth A. Calcium signaling in a narrow somatic submembrane shell during synaptic activity in cerebellar Purkinje neurons. *Proc Natl Acad Sci* USA 92 (22): 10272-6, 1995.

Frick A., Magee JA, Frick J. Magee, Koester HJ, Migliore M, and Johnston D. Normalization of Ca^{2+} signals by small oblique dendrites of CA1 pyramidal neurons, *J Neurosci* 23: 3243–3250, 2003.

Fromherz P, Vetter T. cable properties of arborized Retzius cells of the leech in culture as provbed by a voltage-sensitive dye. *Proc Natl Acad Sci*, USA 89: 204-2045, 1992.

Gardner CR, Walker RJ. The roles of putative neurotransmitters and neuromodulators in annelides and related invertebrates. *Prog Neurobiol* 18:81-120, 1982.

Goodman CS, Heitler WJ. Electrical properties of insect neurones with spiking and non-spiking somata: normal, axotomized, and colchinine-treted neurones. *J Exp Biol* 83: 95-121, 1979.

Gorman AL and Thomas MV. Changes in the intracellular concentration of the free calcium ions in a pace-maker neurone, measured with the metallochromic indicator dye arzenazo III. *J Physiol* 275: 357-376, 1978.

Gorman AL, Thomas MV. Intracellular calcium accumulation during depolarisation in a molluscan neurone. *J Physiol* 308:259-85, 1980.

Gray EG, Young JZ. Electron microscopy of synaptic structure of octopus brain. *J Cell Biol* 21: 87-103, 1964.

Gu X, Muller JK and Young RS. Synaptic integration at a sensory-motor reflex in the leech. *J Physiol* 441: 733-754, 1991.

Hille B. Ionic channels of excitable membranes. *Sundreland, MA: Sinauer*, 1992.

Hockberger PE, Tsen HY, Connor JA. Fura--2 measurements of cultured rat Purkinje neurons show dendritic localization of Ca 2+ influx. *J Neurosci* 9 (7): 2272-84, 1989.

Jaffe DB, Johnston D, Lasser-Ross N, Lisman JE, Miyakawa H, Ross WN. The spread of Na spikes determines the pattern of dendritic Ca entry into hippocampal neurons. *Nature* 357: 244-246, 1992.

Jansen, J. K. S. and Nicholls J. G. Conductance changes, an electrogenic pump and the hyperpolarization of leech neurones following impulses. *J.Physiol.(Lond)* 229: 635-65, 1973.

Kats B, Miledi R. The effect of calcium on acetylcholine release from motor nerve terminals. *Proc. R. Soc. Lond [Biol]* 161: 496-503, 1965.

Khodakhan K, Ogden D. Functional heterogeneity of calcium releas by inositol triphosphate in single Purkinje neurones, cultured cerebellar astrocytes, and peripheral tissues. *Proc Natl Acad Sci* USA 90:4976-4980, 1993.

Koester HJ and Sakmann B. Calcium dynamics associated with action potentials in single nerve terminals of pyramidal cells in layer 2/3 of the young rat neocortex. *J Physiol* 529: 625-646, 2000.

Kostyuk PG. Calcium channels in cellular membranes. J *Mol Neurosci* 2: 123-142, 1990.

Krauthamer V and Ross WN. Regional variations in excitability of barnacle neurons. *J Neurosci* 4:673-682, 1984.

Kristan WB, Jr. Sensory and motor neurones responsible for the local bending response in leeches. *J Exp Biol* 96: 161-180, 1982.

Kristan WB, Mcgirr SJ, Simpson GV. Behavioural and mechanosensory neurone responses to skin stimulation in leeches. *J Exp Biol* 96: 143-160, 1982b.

Kuffler SW, Potter DD. Glia in the leech central nervous system: Physiological properties and neuron-glia relationship. *J Neurophysiol* 27: 290-320, 1964

Levitan I, Kaczmarek L. The neuron, *Oxford University Press*, 1997

Lieberman AR, Webster KE. Aspects of the synaptic organisation of intrinsic neurons in the dorsal lateral geniculate nucleus. An ultrastructural study of the normal and of the experimentally deafferented nucleus in the rat. *J Neurocytol* 3 (6): 677-710, 1974.

Llinas R, Sugimori M. Electrophysiological properties of in vitro purkinje cell dendrites in mammalian cerebellar slices. *J Physiol.* 305:197-213, 1980.

Llinas R, Yarom Y. Properties and distribution of ionic conductances generating electroresponsiveness of mammalian inferior olovary neurons in vitro. *J Physiol* 315:569-584, 1981.

Lockery SR, Kristan WB, Jr. Distributed processing of sensory information in the leech. I. Input-output relations of the local bending reflex. *J Neurosci* 10: 1811-1815, 1990a.

Lockery SR, Kristan WB, Jr. Distributed processing of sensory information in the leech. II. Identification of interneurons contributing to the local bending reflex. *J Neurosci* 10: 1816-1829, 1990b.

Lytton WW, Kristan WB. Localisation of a leech inhibitory synapse by photo-ablation of individual dendrites. *Brain Res* 504: 43-8, 1989.

Macagno ER. Number and distribution of neurons in leech segmental ganglia. *J Comp Neurol* 190 (2): 283-302, 1980.

Markram H, Helm PJ, Sakmann B. Dendritic calcium transients evoked by single back-propagating action potentials in rat neocortical pyramidal neurons. *J Physiol* 485: 1-20, 1995.

Mason A, Kristan WBJr. Neuronal excitation, inhibition and modulation of leech longitudinal muscle. *J Comp Phhysiol* 146: 527-536, 1982.

McClesley EW. Calcium channels:cellular roles and molecular mechanisms. *Curr Opin Neurobiol* 4: 304-312, 1994.

Melinek R, Muller KJ. Action potential initiation site depends on neuronal excitation. *J Neurosci* 16 (8): 2585-2591, 1996.

Muller KJ, Nicholls JG. Different properties of synapses between a single sensory neuron and two different motor cells in the leech C.N.S. *J Physiol* (Lond) 238: 357-369, 1974.

Muller KJ, Nicholls JG, Stent GS. Neurobiology of the leech. Cold Spring Harbor, NY: Cold spring Harbor Laboratory, 1981.

Muller KJ, McMahan UJ. The shapes of sensory and motor neurones and the distribution of their synapses in ganglia of leech: A study using intracellular injection of horseradish peroxidase. *Proc R Soc Lond B* 194:481-499, 1976.

Nicholls JG, Baylor DA. Specific modalities and receptive fields of sensory neurons in CNS of the leech. *J Neurophysiol* 31: 740-756, 1968.

Nicholls JG, Martin AR, Wallace BG. From Neuron to Brain. *Sinauer Associates Inc*., USA, 1992.

Nicholls JG, Martin AR, Wallace BG, Fuchs P. From Neuron to Brain. *Sinauer Associates Inc*., USA, 2001

Norris BJ, Calabrese RL. Identification of motor neurons that contain a FMRFamidelike peptide and the effects of FMRFamide on longitudinal muscle in the medicinal leech, Hirudo medicinalis. *J Comp Neurol* 266:95-111, 1987

Ort CA, Kristan WBJr, Stent GS. Neuronal control of swimming in the medicinal leech. II. Identification and connections of motor neurons. *J Comp Physiol* 94: 121-154, 1874.

Pastor J, Soria BN, Belmonte C. Properties of the nociceptive neurons of the leech segmental ganglion. *J Neurophysiol* 75: 2268-2279, 1996.

Pellegrini M, Simoni A, Pellegrino M. Two types of K+ channels in excised patches of somatic membrane of the leech AP neuron. *Brain Res* 483 (2): 294-300, 1989.

Peterson EL. Visual processing in the leech central nervous system. *Nature* 303: 240-242, 1983.

Peterson EL. Photoreceptors and visual interneurons in the medicinal leech. *J Neurobiol* 15: 413-428, 1984

Pinato G, Battiston S, Torre V. Statistical independence and neural computation in the leech ganglion. *Biol Cybern* 83: 119-130, 2000.

Pinato G, Torre V. Coding and adaptation during mechanical stimulation in the leech nervous system. *J Physiol* 529: 747-762, 2000.

Rall W and Agmon-Snir H. Cable theory for dendritic neurons, in Koch C and Segev I. In *Methods in Neuronal modeling*, sec. ed., MIT Press, Cambridge, MA, ch.2: 27-92, 1998.

Ross W.N and Krauthamer V. Optical measurements of potential changes in axons and processes of neurons of barnacle ganglion. *J Neurosci* 4: 659-672, 1984.

Ross WN, Stockbridge LL, Stochbridge NL. Regional properties of calcium entry in barnacle neurons determined with arsenazo III and a photodiode array. *J Neurosci* 6:1148-59, 1986.

Ross WN, Arechiga H and Nicholls JG. Optical recording of Calcium and voltage transients following impulses in cell bodies and processes of identified leech neurons in culture. *J Neurosci* 7(12): 3877-3887, 1987.

Ross WN, Werman R. Mapping calcium transients in the dendrites of Purkinje cells from the guinea-pig cerebellum in vitro. *J Physiol* 389: 319-36, 1987.

Sabatini BL, Regehr WG. Optical measurement of presynaptic calcium currents. *Biophys J.* 74 (3): 1549-63, 1998.

Sah P, Bekkers JM. Apical dendritic location of slow afterhyperpolarisation current in hypocampal pyramidal neurons: implications for the integration of longterm potentiation. *J Neurosci* 16: 4537-4542, 1996.

Schwindt PC, Crill WE. Modification of current transmitted from apical dendrite to soma by blocade of voltage- and Ca 2+ dependent conductances in rat neocortical pyramidal neurons. *J Neurophysiol* 78: 187-198, 1997.

Shadlen MN and Newsome WT. Noise, neural codes and cortical organization. *Curr. Opin. Neurobiol*. 4:569-579, 1994.

Shadlen, MN and Newsome WT. The variable discharge of cortical neurons: implications for connectivity, computation, and information coding. *J Neurosci*. 18:3870-3896, 1998.

Spruston N, Schiller Y, Stuart G, Sakmann B. Activity-dependent action potential invasion into CA1 pyramidal neuron dendrites. *Science* 268: 297-300, 1995.

Stanley EF, Goping G. Characterisation of a calcium current in a vertebrate cholinergic presynaptic nerve terminal. *J Neurosci* 11 (4): 985-93, 1991.

Stent GS, Kristan WB, Jr., Friesen WO, Ort CA, Poon M, Calabrese RL. Neuronal generation of the leech swimming movement. *Science* 200: 1348-1357, 1978.

Stewart RR, Nicholls JG, Adams WB. Na+, K+ and Ca 2+ currents in identified leech neurones in culture. *J Exp Biol* 141: 1-20, 1989.

Stuart AE. Physiological and morphological properties of motoneurones in the central nervous system of the leech. *J Physiol* 209: 627-646, 1970.

Stuart GJ. and Sakmann B. Active propagation of somatic action potentials into neocortical pyramidal cell dendrites. *Nature* 367: 69-72, 1994.

Stuart GJ, Schiller J. and Sakmann B. Action potential initiation and propagation in rat neocortical pyramidal neurons. *J Physiol* (Lond) 505: 617-632, 1997.

Tsien Rw, Tsien RY. Calcium channels, stores and oscillations. *Annu Rev Cell Biol* 6: 715-760, 1990.

Waters J, Larkum M, Sakmann B, and Helmchen F. Supralinear Ca^{2+} influx into dendritic tufts of layer 2/3 neocortical pyramidal neurons in vitro and in vivo. *J Neurosci* 23: 8558–8567, 2003.

Waters J, Schaefer, A and Sakmann B. Backpropagating action potentials in neurones: measurement, mechanisms and potential functions. *Progress in Biophysics and Molecular Biology* 87: 145-170, 2005.

Wessel R, Kristan WB, Kleinfeld D. Dendritic Ca2+ activated K+ conductances regulate electrical signal propagation in an invertebrate neuron. *J Neurosci* 19: 8319-8326, 1999a.

Wessel R, Kristan WB, Kleinfeld D. Supralinear summation of synaptic inputs by an invertebrate neuron: Dendritic gain is mediated by an "Inward Rectifier" K^+ current. *J Neurosci* 19: 5875-5888, 1999b.

Wittenberg G, Curtis, ML, Adamo SA and William B.Kristan WB. Segmental specialisation of the neuronal connectivity in the leech. *J Comp Physiol* 167 (4): 453-459, 1990.

White JE, Southgate E, Thomson JN, Brenner S. The structure of the nervous system of the nematode Caenorhabditis elegans. *Phil. Trans. R. Soc*. Lond. B 314, 1-340, 1986.

Wodarz A. Establishing cell polarity in development. *Nature Cell Biology* 4, E39-E44, 2002.

Yau KW. Receptive fields, geometry and conduction block of sensory neurones in the central nervous system of the leech. *J Physiol (Lond) Dec*, 263 (3): 513-38, 1976.

Zecevic D, Antic S. Fast optical measurement of membrane potential changes at multiple site of an individual nerve cell. *Histolog J* 30:197-216, 1998.

Zoccolan D, Giachetti A, Torre V. The use of optical flow to characterize muscle contraction. *J Neurosci Methods* 110: 65-80, 2001.

Zoccolan D, Torre V. Using optical flow to characterize sensory-motor interactions in a segment of the medicinal leech. *J Neurosci* 22: 2283-2298, 2002.

Zochowski M, Wachowiak M, Fals C, Cohen LB, Lam Y, Antic S, Zecevic D. Imaging membrane potential with voltage-sensitive dyes. *Biol Bull.* 198: 1-21, 2000.